Alpha-Synuclein: Insight into the Hallmark of Parkinson's Disease as a Target for Quantitative Molecular Diagnostics and Therapeutics

2017

Baggio A. Evangelista
University of Central Florida

ALPHA-SYNUCLEIN: INSIGHT INTO THE HALLMARK OF PARKINSON'S DISEASE AS A TARGET FOR QUANTITATIVE MOLECULAR DIAGNOSTICS AND THERAPEUTICS

by

BAGGIO ANGELO EVANGELISTA

A thesis submitted in partial fulfillment of the requirements
for Honors in the Major Program in Biomedical Sciences
in the College of Medicine
and in the Burnett Honors College
at the University of Central Florida
Orlando, FL

Spring Term, 2017

Thesis Chair: Yoon-Seong Kim

ABSTRACT

Parkinson's disease (PD) is the second-most common neurodegenerative disease after Alzheimer's disease. With 500,000 individuals currently living with Parkinson's and nearly 60,000 new cases diagnosed each year, this disease causes significant financial burden on the healthcare system - amassing to annual expenditures totaling 200 billion dollars; predicted to increase through 2050. The disease phenotype is characterized by a combination of a resting tremor, bradykinesia, muscular rigidity, and depression due to dopaminergic neuronal death in the midbrain. The cause of the neurotoxicity has been largely discussed, with strong evidence suggesting that the protein, alpha-Synuclein, is a key factor. Under native conditions, alpha-Synuclein can be found localized at synaptic terminals where it is hypothesized to be involved in vesicle trafficking and recycling. However, its biochemical profile reveals a hydrophobic region that, once subjected to insult, initiates an aggregation cascade. Oligomeric species—products of the aggregation cascade—demonstrate marked neurotoxicity in dopaminergic neurons and illustrate migratory potential to neighboring healthy neurons, thereby contributing to progressive neurodegeneration.

The current golden standard for PD diagnostics is a highly qualitative system involving a process-by-elimination with accuracy that is contingent upon physician experience. This, and a lack of standardized clinical testing procedures, lends to a 25% misdiagnosis rate. Even under circumstances of an accurate PD diagnosis, the only treatment options are pharmacologics that have a wide range of adverse side effects and ultimately contribute to systemic metabolic dysfunction. Thus, the research presented in this thesis seeks to overcome these current

challenges by providing (1) a quantitative diagnostic platform and (2) a biomolecular therapeutic, towards oligomeric alpha-Synuclein.

Aim 1: serves as a proof-of-concept for the use of catalytic nucleic acid moieties, deoxyribozymes and aptamers, to quantify alpha-Synuclein in a novel manner and explore the ability to detect oligomeric cytotoxic species. The cost-effective nature of these sensors allows for continued optimization.

Aim 2: serves to establish a potential therapy that can abrogate alpha-synuclein oligomerization and toxicity through use of a modified Protein Disulfide Isomerase (PDI) peptide when introduced to live cells treated to simulate pre-parkinsonian pathology.

DEDICATION

This thesis, in its entirety, as well as any advancements in neurodegenerative medicine from which may rise, are dedicated to my late grandfather, Carmine Roberto and all others with Parkinson's disease who suffer in silence; they have not gone unnoticed.

ACKNOWLEDGMENTS

I would like to extend my deepest gratitude to my thesis chair, Dr. Yoon-Seong Kim for welcoming me into his lab, seeing potential in me that I did not know I had, and allowing me to think as an independent scientist shortly after joining. To his lab members, Subhrangshu Guhathakurta, Goun Je, Sambudda Basu, Levi Adams, and Eugene Bok, for assisting me throughout this process. To Dr. Kenneth Teter, for welcoming me into his lab and lending continuous academic support and career guidance. To Dr. Dmitry Kolpashchikov, for welcoming me into his lab and contributing financially to this research. To Dr. Robert Borgon and Professor Nicole Verity, for years of guidance, assistance, and provision of invaluable knowledge and skillsets. To my esteemed colleague, Ashelyn Sidders, for her assistance with data processing and unending support as a friend. To my lifelong friends, Christopher Biles, Sheryl Esmond, and Katrina Pham for their endless motivation at the highs and lows of this work. Finally, to my parents, Marcello and Italia Evangelista, for without their support none of this would be possible. Thank you.

TABLE OF CONTENTS

LIST OF FIGURES

LIST OF TABLES

CHAPTER ONE: INTRODUCTION

Etiology of Parkinson's Disease

Parkinson's disease (PD) is a progressive neurodegenerative disease with incidents making it the second most common neurodegenerative disease after Alzheimer's disease[1]. The disease phenotype is characterized by any combination of four diagnostic features: resting tremor, bradykinesia, muscular rigidity and postural instability due to dopaminergic deficit in the nigrostriatal region of the midbrain[2]. Current epidemiological data reveals that, as of 2005, more than 4 million were diagnosed worldwide, with a 0.3% prevalence in the general population and a male:female ratio of 3:2[1]. The general cause of PD is unknown and largely debated, as both idiopathic and genetic forms of the disease arise in the clinical setting. Diagnosis and treatment of PD are limited, likely due to the inherent difficulty in delineating several near-identical symptom profiles found in other neurodegenerative diseases[3]. Much attention in regards to targeted diagnostics and therapies has been turned to a key molecular hallmark of PD, alpha-Synuclein (α-SYN), which exists as aggregated intraneuronal inclusions in the PD brain[4].

Clinical Diagnosis of PD

As previously mentioned, the cause of PD is elusive, with early and/or prophylactic diagnosis remaining a challenge during pathogenesis[5]. Genetic screening is available but is only applicable in a limited number of cases[6], excluding idiopathic conditions, which are more epidemiologically prevalent. It has been noted that environmental, genetic, and epigenetic influences can be responsible for an individual's propensity to PD at varying ages in life. Typically, the disease

occurs infrequently under 40 years of age, coined *familial* PD. It is most prevalent in patients over 65 years of age, clinically denoted as *idiopathic* PD. In the United States alone, there exists an excess of 500,000 patients, with 60,000 new patients diagnosed yearly[7].

As mentioned above and described below, motor characteristics denote a symptomatic patient in the clinical setting.

1) Bradykinesia is defined as the loss of speed in performing repetitive movements of extremities, and is easily confused with simple slowness encountered during advanced age. A subset of bradykinesia can include any combination of *hypomimia, hypophonia*, *micrographia,* and *dysphagia* (decreased or absent facial expression, diminutive vocal projection, diminutive handwriting, and difficulty swallowing, respectively)[2].

2) Resting tremor, otherwise known as *parkinsonian tremor*, is the presentation of subtle, rhythmic movements when the body is not engaged physically or mentally. The most notorious clinical example of resting tremor is known as "pill-rolling" in which the patient involuntarily rubs the flat of their pollex and index finger together in minute circular patterns[8].

3) Rigidity is classified as an abnormal increase in muscle tone during movement of the both flexor and extensor muscular analogs, in either the neck or extremities. This incongruity amongst muscle groups leads the patient to experience "cog-wheel" movements where movement in one muscle group will trigger simultaneous movement of another group that otherwise would not be integrated[9].

4) Gait Impairment is the final and most identifiable symptom of a PD patient. Often, the patient will exhibit "anterior truncal flexion" whereby the upper body leans inward, less than 20 degrees relative to normal. This is accompanied with shuffling footsteps where the feet of a patient will not undergo dorsal flexion or plantar flexion during walking. To conclude gait impairment, a physician will employ a "pull-test" to gage the individual's ability to maintain a stable posture or observe a sort of "chasing" of their center of gravity[10].

In conjunction with the four motor criteria, patients will also exhibit non-motor symptoms linked to neuropsychiatric, autonomic, and sensory deficits such as anxiety, hyperlacrimation, insomnia, and hyposmia[11]. Such symptoms are often disregarded in the absence of motor deficits, which has the potential to lead to misdiagnoses and, as a result, imposes a large degree of physician-to-physician variability due to the strict clinical nature of PD diagnosis. Studies have shown that correct diagnosis of PD in cases where classic symptoms are absent is challenging for physicians. Autopsy data have shown 24% of individuals initially diagnosed with PD lacked specific hallmarks of the disease (i.e. Lewy Bodies) and actually had diseases more aptly classified as progressive supranuclear palsy, Alzheimer's disease, or multiple system atrophy[12]. Furthermore, data suggest diagnoses can occur anywhere from two months to 18 years after symptom onset, with 5-25% of diagnosed patients having been misdiagnosed and receiving medication for a disease they did not in fact have[13]. Conversely, it has been reported that 20% of patients who received clean bills of health due to the lack of "gold-standard" symptoms, did in fact have PD[3]. The current state of diagnosis for PD, without a ubiquitous and quantifiable target, has proven to be imprecise.

Much attention has been turned to monitoring the depreciation of dopamine in the Substantia Nigra (SN), a key factor in PD responsible for the discordant fine-motor processes. For several decades, post-mortem analysis of the striatum (projected upon by the SN) has revealed a striking depletion of dopamine in PD patients (Figure 1). Through positron emission tomography and single-photon emission computed tomography (PET and SPECT, respectively), radio-ligands such as [^{99m}Tc]TRODAT-1 SPECT and [^{18}F] DOPA PET are able to target dopamine transporters either at the pre- or post-synaptic termini. This allows physicians to quantify with high specificity the concentration of dopamine in the SN and subsequent discrimination between PD and non-degenerative diseases[14]. However, there is a major limitation to dopaminergic molecular imaging: the sensitivity and specificity of imaging is based on the previously discussed "gold-standards" of clinical PD diagnosis, which at this point are understood to be quite variable. As such, further expansion on current imaging protocols would be established on what is previously understood as a vacuous clinical foundation. Therein lies a continued need to establish biomarkers that can both reduce chances of misdiagnoses as well as provide substantial and quantitative data that distinguishes between Parkinson's-like diseases such as non-Lewy Body dementia and non-degenerative tremor disorders. Patient samples such as blood or cerebral spinal fluid are of increasing interest as a timely means of detection. However, due to multi-variable experimentation, these approaches are quire premature and therefore require more exploration[15].

Current Clinical Treatment of PD

To date, several interventions of PD, both pharmacological and surgical, exist to a semi-efficient degree, making therapeutics higher in terms of clinical competency when compared to diagnostics. However, a substantial amount of adverse effects arise from both, regardless of the strict guidelines physicians follow to ensure proper treatment. From the pharmacological perspective, subclasses include: Levodopa, Catechol-o-methyl-transferase (COMT) inhibitors, dopamine agonists, and non-dopaminergic drugs.[16].

Levodopa (L-DOPA), or L-3,4-dihydroxy-phenylalanine, is a chemical analog of dopamine. Because dopamine has a terminal amine conserved from its amino acid precursor, tyrosine, its highly polarized dipole-moment inhibits the ability to penetrate the blood-brain-barrier (BBB) and, as such, cannot be used as a drug with the aim of compensating for the decline of intrastriatal dopamine[17]. Levodopa, however, maintains its amino-acyl backbone and is able to permeate the BBB. After crossing the BBB, DOPA decarboxylase then reduces the carboxy terminus of levodopa to a secondary amine, yielding intracerebral dopamine. Despite it being the most popular, as well as potent pharmacologic available for PD, L-DOPA in itself can induce motor pathologies such as dyskinesias. L-DOPA is therefore in a constant state of debate regarding its clinical efficacy[16]. At times, a peripheral DOPA-decarboxylase inhibitor, carbidopa, enhances the drug's potential by limiting the activity of DOPA-decarboxylase in regions of the body other than the brain. It has been reported that patients prescribed L-DOPA will typically experience motor deficits after five years of regimented L-DOPA, which leads some physicians to withhold L-DOPA therapies until deemed fit so as to postpone the onset of the adverse side effects. It has also been noted that early-onset PD, as well as genetic forms such as PARK2 and

PARK8, are especially susceptible to the development of L-DOPA-related motor deficits[18]. Countermeasures for the amelioration or prophylaxis of L-DOPA dyskinesias include titration of the dosage, additional medications, or even surgical intervention to place drug-secreting bioreactors in localized area of the brain.

Catechol-o-methyltransferase (COMT) is an enzyme that is responsible for the degradation of catecholamines such as dopamine, norepinephrine, and epinephrine. In doing so, a catechol hydroxyl group is methylated, and subsequently converted to the metabolite, Homovanillic acid (HVA through the enzymatic activity of monoamine oxidase (MAO). HVA is excreted in the urine. The inhibition of COMT thus blocks the degradation of both endogenous dopamine and L-DOPA, thereby increasing the plasma concentration of L-DOPA and prolonging its activity, while reducing the aforementioned side-effects of L-DOPA-induced dyskinesias[19]. A stark drawback to certain COMT inhibitors is the necessitation of stringent clinical monitoring due to the hypervariable tolerability of the drugs. A 2007 study indicated that a 100 mg dose of COMT inhibitor three times daily increased hepatotoxicity, with liver transaminase levels almost three times the upper normal limit (UNL), in some cases[20]. With that, individuals prescribed COMT inhibitors are required to have liver enzyme monitoring approximately every two weeks for the first year of the regiment.

Dopamine agonists are typically administered in the initial period of PD as they allow physicians to delay the use of L-DOPA and its adverse effects[21]. Dopamine agonists do not require further metabolic processing by the body and are able to bypass dopamine synthesis at the pre-synaptic termini[22]. Upon binding to D2 receptors, antiparkinsonian effects can ensue; however, engagement of the D1 receptor is also necessitated to mediate behavioral deficits.

Unfortunately, the overall ameliorative effects are quite modest with respect to the L-DOPA counterpart, and, as with COMT inhibitors, can involve a degree of hepatotoxicity from its pharmacokinetic profile.

Non-dopaminergic pharmacologics include anticholinergics which have been shown to mediate symptoms in the early years of PD, and are often employed in patients of a younger demographic that display advanced motor impairment. To counter PD-induced behavioral issues such as depression, neurologists also prescribe anticholinergics that enhance pre-synaptic serotonergic, 5HT2 and 5HT3, receptors. Drawbacks to such medications include cognitive impairment and incontinence, further perpetuating the theme of non-specific means of PD treatment and the adverse side-effects implicated at the peripheral level[23].

Advents in molecular biology have yielded several in-trial biologics for restorative and protective properties at the midbrain. At the in vitro level, neurotrophic factors such as neurturin (NTN) and glial cell-line-derived neurotrophic factor (GDFN) have demonstrated prophylactic effects on the dopaminergic neurons by preventing cell-death[24,25]. This observation, however, was not at the patient level as intracerebroventricular injection of GDFN in a human trial led to severe dementia and anorexia without ameliorating the effects of PD. More recently, a twelve patient study involved stereotaxic implantation of an adeno-associated virus type 2 vector (AAV2-NTN) that utilized a patient's transcription and translation machinery to produce intraputaminal NTN. This work showed an improvement in the Unified Parkinson's Disease Rating Scale (UPDRS) by upwards of 20%. Further investment was made in the use of retinal pigment epithelial cells (hRPE), which are responsible for the production of L-DOPA in the retina. Stereotactic implantation of hRPE demonstrated symptom improvement in human

subjects, improving UPDRS by upwards of ~50%[26]. It should be noted, however, there are substantial drawbacks to the use of aforementioned technology. Stereotaxic surgery is an invasive procedure, and the exact location of injection varies from human to human, only conserved within several cubic millimeters based on the x,y,z coordinate system. Furthermore, the use of recombinant DNA or immortalized cells are topics of heated debate, requiring substantial amount of financial investment and insurance, FDA approval, and a timely exploration of methods to control the potential adverse side-effects on a systemic level.

Alpha-Synuclein Mediated Molecular Pathogenesis

Structure of Alpha-Synuclein

A hallmark feature of PD is the intraneuronal presence of Lewy Bodies; cytoplasmic inclusions of aggregated α-SYN[27] (Figure 2). This low molecular weight (14 kDa) protein is a subclass of synuclein proteins along with beta- and gamma-Synuclein, although its beta and gamma relatives are not associated with progressive neurodegeneration[28]. In non-pathological conditions, this protein is highly soluble and abundant in regions of the brain, predominantly in the presynaptic terminals of the neocortex, hippocampus, striatum, thalamus, and cerebellum. It is also found elsewhere in the body, such as liver and bowel, albeit at lower concentrations. Structural analysis reveals it is comprised of random coils in its natively unfolded state and can withstand temperatures of 110°C as well as highly acidic environments, leading scientists to postulate PD as prion-mediated pathogenesis[29]. Upon insult, soluble monomers undergo aggregation with the potential to inflict cytotoxic effects on neurons by compromising their membrane integrity. The 140 amino acid sequence of α-SYN has been largely studied, and thorough analysis reveals the

presence of three conserved domains including 1) a highly conserved N-terminal repeat domain, 2) a central hydrophobic domain, termed non-Aβ component (NAC) and 3) an acidic carboxy-terminal domain (Figure 3).

1) N-terminal Repeat Domain: consists of residues 1 through 65. This region has six copies of 11 imperfect amino acid repeats based on a "Lys-Thr-Lys-Glu-Gly-Val" consensus sequence that contributes to the formation of two alpha-helical structures[30]. The presence of both hydrophobic and hydrophilic R groups manifest into an amphipathic lipid-binding domain that allow this region to engage the negatively charged lipids of the phospholipid bilayer, constituting a membrane-associated construct[31]. It is believed that its lipid-associated interactions may potentiate α-SYN's aggregative properties in neurodegenerative pathophysiologies. It is also within this region that two point mutations have been elucidated as precursors to autosomal dominant early-onset PD: Ala at position 53 to Thr (A53T) and Ala at position 30 to Pro (A30P). Both mutations confer a beta-sheet conformation that facilitates α-SYN oligomerization[32].
2) NAC domain: Residues 65-95, confer to the highly amyloidogenic region of the molecule. These amino acids are also deemed responsible for the protein's ability to shift from random coil to β-sheet moiety, facilitating the genesis of amyloid oligomers, protofibrils, and fibrils characteristic of PD and Alzheimer's disease[33].
3) Acidic Carboxy-Terminal Domain: Residues 96-140 are highly variable in sequence and length, however conserve highly negatively charged acidic amino acids[34]. This region does not contribute to higher-ordered secondary structures but nevertheless

confers a chaperone-like property to α-SYN[35]. Truncations of these residues have demonstrated significantly heightened aggregation potential. Several phosphorylation sites mediate the chaperone-like activity through involvement of tyrosine kinase as a putative anti-neurodegenerative property[36]. Post-mortem analysis of purified LBs illustrates the presence of full-length α-SYN in conjunction with fragments having truncated acidic carboxy-terminal domains[37].

Physiological Role of α-SYN

Extrapolations based on the structural analysis of α-SYN are indicative of several physiological roles, although a definitive normative process has yet to be confirmed. It is believed that a major role utilizes the aliphatic N-terminal repeat domain to engage presynaptic neurons in vesicular neurotransmitter release[38]. Bovine studies suggest α-SYN as an inhibitor of phospholipase D_2, which facilitates the hydrolysis of phosphatidylcholine to phosphatidic acid (PA). PA, a macromolecular phospholipid building block, constitutes vesicular bilayers implicated in exocytotic neurotransmitter secretion in conjunction with vesicle recycling and neurotransmitter turnover. Therefore, an inhibition of PA has an immediate inhibitory effect on the production of neurotransmitter packaging. In α-SYN knockout mice, stimulation of the substantia nigra pars compacta results in an exhaustive release of dopamine from pre-synaptic terminals, suggesting a negative regulatory role for α-SYN to conserve dopamine reservoirs[39].

α-SYN's acidic carboxyl-terminal domain and various phosphorylation sites therein have substantiated the notion of an inherent chaperone-like quality to inhibit protein aggregation and assist in the re-folding of non-native proteins. Approximately 40% of α-SYN is homologous to

the molecular chaperone 14-3-3, which is abundant in the soluble protein fraction of the brain. However, 14-3-3 is detected in post-mortem analytes of LB's extracted from the SN. With that, it is hypothesized that α-SYN infarcts 14-3-3's ability to alleviate aggregation-induced cytotoxicity, ultimately compromising the cellular integrity[40].

α-SYN Pathogenesis

As previously mentioned, PD is likely the result of imposed dopaminergic cytotoxicity due to the presence of intracytoplasmic inclusions of α-SYN. α-SYN, otherwise monomeric in a non-pathological state, forms insoluble higher-order aggregates that likely compromise the integrity of the plasma membrane leading to progressive neurodegeneration (Figure 4). In vivo models support this hypothesis by having demonstrated that the addition of aggregated, pre-fibrillar forms (PFF) of α-SYN induced cell-death after ~120 days of inoculation. Also discovered was a self-propagating cascade of wild-type α-SYN aggregation in adjacent cells, illustrated by the presence of intracellular punctations of α-SYN via immunocytochemistry[29]. At the mammalian level, stereotaxic injection of α-SYN PFFs in-vivo demonstrated extreme toxicity and synaptic impairment in rat models with the presentation of PD-like symptoms. The mechanism by which α-SYN undergoes insult and subsequent aggregation has therefore been a great focal point for PD etiology. Two competing proposals for aggregation include 1) malfunctions in the ubiquitin proteasome system (UPS) and 2) oxidative stress induced by free radicals and reactive oxygen species (ROS).

1) UPS is the primary biochemical mechanism by which cells degrade and recycle both normal as well as abnormal intracellular proteins through a two-step signaling

cascade. A protein targeted for degradation will be acted upon by several ubiquitin-conjugating enzymes, through which interaction with the 26S proteasome will occur[41]. Interaction and recognition of the ubiquitin tags induces ATP-dependent proteolysis within the 20S core cylindrical unit, releasing small peptide fragments from the 19S cap to be further degraded in the cytosol via transaminases and transpeptidases[42]. The cascade is completed upon release of reusable ubiquitin components. Failure or downregulation of the UPS can cause an intracellular congestion of proteins intended for degradation and is implicit in the beginnings of neurodegeneration. Post-mortem analysis of the Substantia Nigra pars compacta LBs reveals the presence of ubiquitin polymers as well as fragments of the 26S proteasome. Biochemical analysis reveals proteins tagged for degradation bear ubiquitin tags, suggesting that poly-ubiquitination contributes to an inefficacious degradation pathway and subsequent PD pathogenesis[43].

2) The presence of oxidants has been well established as a method by which protein insult occurs. In vitro, it has been demonstrated that exposure of α-SYN to hydrogen peroxide and iron facilitates the aggregation of higher-ordered structures and formation of cytotoxic intermediates[44]. In a process coined the Fenton effect, cultured cells treated with traces of ferrous chloride demonstrate a heightened aggregation potential evident through Western blotting, immunocytochemistry, and cytotoxicity assays. Similar results are seen through use of hydrogen peroxide with the added effect of ROS-mediated mitochondrial dysfunction and cell death[45]. Studies involving mutated α-SYN (A53T, S42Y, A30P) illustrated a hyper-susceptible aggregation

response to oxidative species. The proposed mechanism by which oxidation-induced aggregation in PD occurs involves the chemical nature of dopamine. An inherent free-radical generator, as well as principal neurotransmitter in the SN, dopamine's reactive chemical nature is compounded by free radical-generating iron which accumulates in neurons with advancing age, and substantiates a likely hypothesis as a pathogenic mechanism[46]. Advances in studying this process in vivo are being made to avoid the commonly used potent environmental toxins MPTP, Paraquat, and Rotenone, which induce neuronal death faster than LB formation[47].

While a definitive physiological role and mode of pathogenesis remains speculative in relation to the biochemical properties of α-SYN, the distinction between the monomeric and aggregated ultrastructure potentiates a clinically applicable biomarker for LB-related synucleinopathies such as PD. Researchers have applied antibody-based detection methods (ELISA, dot blots, etc.) to quantify α-SYN from patient samples. However, because antibodies are sequence-specific, differentiation between monomeric and oligomeric species has proven difficult. Recent advancements in oligonucleotide chemistry suggest small DNA constructs, or aptamers, can be used to identify macromolecules in an antibody-like fashion with the added benefit of distinguishing between polymorphic species.

Aptamers

Aptamers are receiving a significant amount of scientific exploration at the academic and industrial level as a class of functional nucleic-acid compounds with wide-scale applications targeted toward the clinical setting. Aptamers are composed of synthetic ssRNA or

ssDNA,which, due to intra-nucleic acid hydrogen bonding, achieve higher-ordered secondary and tertiary structures that confer a functional "lock-and-key" property to specific substrates in an antibody-like fashion[48] (Figure 5). A functional aptamer ranges in size from ~20-100 nt, comparatively 20-25 fold smaller than the monoclonal antibody analogs, allowing for an increased penetrable ability across a variety of biological membranes and barriers such as the Bowman-Glomerular Capsule interface[49]. Furthermore, these moieties are nucleic acid polymers rather amino acid derived, reducing the chance of immunogenic response in vivo. Unlike antibodies, can distinguish between structural variants of proteins such as monomers and oligomers, whole-cells, or tissues; qualities that make aptamers substantial technology for use in clinical applications such as diagnostics, therapeutics, or synergistic "theranostics"[50].

Synthesis

Aptamer synthesis was well established in 1990. However translational applications were not possible until recently when intellectual property patents on the mode of synthesis expired, leading to a surge of aptamer-based research. Biochemists Tuerk and Gold coined the process Systematic Evolution of Ligands by Exponential enrichment (SELEX) as they sought to select a library of RNA ligands that interacted with T4 DNA Polymerase[51] (Figure 6). This iterative process begins with a randomized library of oligonucleotides, or "oligos" linked to a ubiquitous priming region. The oligos are heated in folding buffer that contains 1 mM $MgCl_2$ to 95°C to denature the oligos and disrupt randomized intramolecular binding. The solution is then allowed to cool to room temperature at approximately 1°C per minute, which through Mg^{2+} cofactor, creates a functional aptamer by allowing the oligo to self-anneal according to the most

energetically favorable secondary or tertiary structure. The randomized aptamers are then incubated with target antigens as well as counter-selection compounds[52]. Those sequences that interact with counter-selection compounds are discarded while those that demonstrate binding to the target compound are amplified via PCR or RTPCR (for RNA moieties) with primers that anneal to the ubiquitous priming regions in the oligo library. This selection and amplification process is then repeated 10-20 times. Final selection will yield several aptamers with conserved sequences but variable dissociation constants as determined by surface plasmon resonance. This process can also be carried out using live cultured cells as a *de novo* process through which novel biomarkers can be established for specific cell types. Advantages of SELEX compared to animal-mediated antibody production include efficient production scaling, reduced production time, and a predictable chemical nature that allows for homogenous conjugation to fluorophores, quenchers, and drug cargo[50]. Furthermore, aptameric sequences can be adapted for a DNA-based enzymatic analyte detection system, or deoxyribozyme, to increase sensitivity and improve limits of detection.

Deoxyribozyme Sensors

Deoxyribozymes (Dz) are a class of novel synthetic oligonucleotide catalytic moieties that can be used in vitro to detect specific analytes including: metals, small molecules, and nucleic acids, with lower limits of detection than traditional means. This is established through Dz's enzyme-kinetic properties, which allow for signal accumulation and optimization based on incubation temperature, construct concentration, and incubation time.

Kolpashchikov et al have been developing binary Dz sensors (BiDz) for the detection of polymorphic *Mycobacteria* DNA fragments as a means of a small-scale, affordable, and technologically simple diagnostic aid[53]. In their design, two non-natural DNA strands hybridize to either RNA or DNA fragments of *M. tuberculosis*, through traditional base pairing. Upon hybridization, a catalytic loop is formed through which phosphodiester cleavage of a Black Hole-RNA-Fluorescein sequence substrate (F_sub) is permissible. This cleavage allows for detection via fluorimetry at 517 nm (Figure 7). The technology allows for 1) highly sensitive and 2) specific mode of detection, both of which are inherent requirements for biosensors:

1. Because this system adheres to traditional enzyme-kinetic laws, the sensitivity of BiDz to the target antigen or analyte can be optimized to achieve significant detection even in low abundance (pM or fM) by altering the concentration of BiDz constructs, the concentration of F_sub, incubation time, and temperature of incubation (30°C, 37°C, 55°C, 65°C). This establishes a signal amplification feature required to achieve a robust limit of detection (LOD), without PCR-based amplification methods.
2. The BiDz system reduces the occurrence of non-specific interactions due to the necessitation for both constructs to be sufficiently interacting with analyte in order to establish a functional catalytic core. This prevents weak interactions from contributing to signal production as may be the case with traditional fluorescent labeled probes[54].

To further improve LOD, *Kolpashchikov et al* has communicated a three-dimensional DNA scaffold, or DNA antenna tile-associated Dz sensor (Figure 8). With this, nine

oligonucleotide sequences with intrinsic self-complementarity are annealed to form a planar "tile", upon which one of the two BiDz, and a "hook" sequence, which is partially complementary to each of the nine scaffolding sequences and partially complementary to the F_sub sequence or a modified aptamer sequence, are also annealed. This is an adaptation of the Chou model, wherein proteins can "channel" substrate to the active sites of the protein to increase diffusion-controlled catalysis and product formation. The hook sequences will therefore draw F_sub molecules out of solution toward the catalytic BiDz site and increase signal output, thereby broadening the LOD. Furthermore, the intricate scaffolding system of the Dz tile allows for the caging of drug cargo; conferring both diagnostic and therapeutic properties to this technology. A final Dz configuration includes aptamer Dz systems wherein an entire aptamer sequence is linked to each catalytic segment (Figure 9). Because of the ease of synthesis of these oligonucleotides (identical to oligonucleotide primer synthesis and purification), as well as the ubiquitous nature of the catalytic and tile sequences, one needs to simply supplement their desired sequence for the analyte binding arms to make use of the Dz systems. Although the BiDz, and Tile-BiDz systems have shown success for detecting nucleic acids, there are no known studies to date for the detection of protein analytes. However, with much advancement in aptamer-mediated protein detection, their use in Dz systems is imminent[55].

In-Vivo Applications

Aptamers intended for in vivo applications must be chemically modified to withstand dynamic biological conditions not otherwise encountered in in vitro assays. A drawback to aptamer chemistry is degradation of the uncapped 5' and 3' termini upon interaction with exonucleases.

Furthermore, the phosphodiester backbone in pyrimidine residues can be targeted by ribonucleases, leading to internal degradation and loss of functional conformation. However, through the use of modified nucleotides, the stability of aptamers for in vivo studies can be efficiently, and cost-effectively, ameliorated. Inverted 2'-o-modified pyrimidine nucleotides such as 2'-amino pyrimidines and 2'-fluoro pyrimidines render endo/exonucleases catalytically inactive[56]. It is imperative that inverted bases as well as high molecular weight cargos be incorporated into the oligo library before SELEX as the modifications can alter dissociation constants or even specificity due to intramolecular interactions conferring altered Gibb's free energies and conformations[57].

The first aptamer to receive FDA approval occurred in 2004. To date several aptamers have approached clinical trial as modes of molecular imaging, diagnostics, and therapeutics. Popular fields of application include cancer therapy and arterial heart disease. ARC1779 was developed as a DNA aptamer selected for interaction with von Willenbrand (vWF) factor. Binding to vWF imposes an electro-repulsive force that inhibits ligand interaction with platelet membrane receptors. This then hampers the arterial thrombogenic cascade and formation of atherosclerotic plaque deposits, which could serve as a means of mediating coronary artery disease[58]. A similar mechanism is employed in cancer therapies wherein ARC1905, an RNA aptamer, binds complement component 5 (C5) and inhibits formation of the Membrane-Attack Complex (MAC). Absence of the MAC leads to down regulation of cell lysis and stunting of vascular-endothelial growth factor, hampering tumor angiogenesis and metastasis. Areas of interest such as cancer and vascular pathologies are applicable for aptamer studies due to the relative ease of access to targets as well as little variability among antigens[59].

Further advancements in aptamer technology and synthesis have led to the development of highly functional aptamer probes that exhibit intrinsic activation properties upon interaction with their targets. TLS11a-GC was developed as a DNA aptamer via whole-cell SELEX and is able to recognize entire hepatocellular carcinoma cells. Utilizing aptamers' intrinsic base-pairing principle, scientists successfully incorporated the anticancer drug Doxorubicin (DOX), which intercalates DNA, with an aptamer targeting only cancerous tissue. Therefore, instead of administering DOX systemically, which has had implications of induced cardiomyopathy, the drug can be delivered within the aptamer and released upon target-specific interaction[60]. Similarly, Activatable Aptamer Probes (AAP) are synthesized to have a fluorophore and quencher in close proximity when in the unbound state. Upon binding to their targets, a conformational shift induces dissociation of the quencher, permitting excitation and emission of the fluorophore. An interdisciplinary field, coined theranostics, utilizes this technology as a means of both diagnostics and therapeutics in the form of a chimera. Specifically, upon target binding and dissociation of the quencher in AAPs, the fluorescence emission can be used as a molecular imaging moiety, but also an excitatory frequency to a nearby substrate such as gold nanoparticles (AuNPs). Excitation of the AuNPs results in an immediate release of localized thermal energy used to destroy cancerous tissue in a controlled fashion without damaging the nearby healthy tissue, or photothermal therapy (PTT)[61].

Within the past five years, a considerable amount of study has been invested with the aim of surmounting the limitations to aptamer-based neurodegenerative diagnostics and therapeutics including:

1) *Biomarkers for neurodegenerative diseases are often higher ordered structures of peptides that are nevertheless found in monomeric states in non-pathoogical conditions and therefore are composed of identical chemical sequences that must be differentiable by the molecular probe*

Ikebukuro et. al has demonstrated the production of aptamers selected for oligomeric α-SYN only. Using the typical SELEX scheme, the aptamers were counter-selected against monomeric and fribrillar forms, so as to enable researchers to detect the presence of cytotoxic species before LB production and subsequent neurodegeneration occur. Biochemical analysis via TfT analysis suggests aptamers T-SO517 and T-SO606 produce detectable responses against immobilized α-SYN only when TfT intensity surpasses 1000 A.U., indicating the presence of higher-ordered species. Aptamer T-SO508, while showing the strongest reaction to oligomeric α-SYN, also detected Aβ due to the conserved beta-edge conformation. However, because this type of motif is present in a wide variety of proteins (IgG, CRP, albumin), a sufficient negative selection is necessary to produce highly specific probes for use in physiological environments[52].

2) *The blood-brain-barrier (BBB) inhibits upwards of 80% of polar, charged molecules such as DNA*

The BBB is a major hurdle in diagnosing and treating neurodegenerative diseases. While several drugs and probes have shown promise at the neurological level, achieving their final destination in a non-invasive manner leaves room for improvement[62]. In 2014, Freskgard et. al demonstrated increased brain penetration of a therapeutic monovalent antibody for Aβ plaques (mAb31) achieved through monovalent engagement of the Transferrin receptor (TfR). Engagement of this

receptor at the BBB microvasculature allows for receptor-mediated transcytosis through the polarized endothelium, delivering cargo through the abluminal region into the cerebral parenchyma. Within 15 minutes, intravenous injection of the antibody chimera displayed marked penetration and plaque decoration. Approximately 4.5 months post-treatment of the PS2APP amyloidosis mouse model, there was an increased therapeutic effect in the reduction of plaques 8-16 μm^2 when compared to treatment without TfR engagement. This study shed light on the significance of receptor engagement for non-invasive shuttling across the BBB. However, antibody-based reactions of the TfR and parenchymal delivery can impose several disadvantages such as intra-endothelial lysosomal sorting and degradation upon divalent interaction of the receptor or an induced immunogenic reaction as a result of the large peptide-based IgG molecules[63]. Beltram et. al utilized a similar concept of TfR engagement as a means of CNS delivery but employed the anti-TfR aptamer ATTO 633 as opposed to antibodies. Because aptamers display monovalent modes of binding, there is a reduced chance of lysosomal sorting at the BBB endothelium[64].

3) Biomarkers for neurodegenerative diseases, such as α-SYN aggregates, are intracellular inclusions, therefore aptamers must be capable of freely accessing the plasmalemma

Because α-SYN deposits are intracellular, another hurdle to engage the LB for diagnostic and/or therapeutic purposes is the ability and efficiency by which molecular probes can diffuse through the neuronal plasma membrane without imparting their own degree of cellular damage after CNS access. Further metabolic differences between neurons and the polarized endothelium of the BBB necessitate conflicting functions of the molecular shuttle. In endothelium, or BBB

interface, maintenance in the transport vesicle is imperative to be completely transcytosed across the BBB. However, at the neuronal interface vesicular release into the cytoplasm is required for interaction with the cytosolic target in a process dubbed endosomal release. Battaglia et. al illustrated engagement of Low Density Lipoprotein Related Protein 1 (LRP-1) receptor facilitates the aforementioned requirements. pH-sensitive polymersomes containing nucleic acids, coated with LRP-1 ligand Angiopep-2, triggers transcytosis at the BBB endothelium. Once in the parenchyma, these constructs are then able to engage in traditional endocytosis by the neurons without intracellular lysosomal sorting and circulate freely in the cytoplasm of the neurons. Advancements in aptamer- and nanotechnology have established several modes by which diagnostic or therapeutic aptamers can self-facilitate target engagement with minimally invasive and diminutive toxic effects in vivo[65]. It can be understood, however, that the significance of the information provided to a patient by a quantitative diagnostic is contingent upon the therapeutic alternatives available thereafter. Because of this, a target-specific therapeutic that obstructs neuropathy at the mechanistic hallmark of PD progression—α-SYN aggregation—is necessary. Recent discoveries with Protein Disulfide Isomerase are suggestive of a potential biologic that ameliorates α-SYN aggregation and thus lends a therapeutic route of exploration.

Protein Disulfide Isomerase

Protein Disulfide Isomerase (PDI) is a ubiquitously expressed 55 kDa thioreductase, with oxidoreductase, isomerase, and chaperone-like properties[66]**.** A Lys-Asp-Glu-Leu (KDEL) retention sequence localizes PDI predominantly in the endoplasmic reticulum (ER) where post-

translational packaging, modification, and folding occur. However, PDI has been located in the intracytoplasmic and extracellular regions as well[67,68]. PDI is responsible for the formation, removal, and rearrangement of covalent disulfide bonds as part of the tertiary folding process of nascent proteins[69]. Several pathophysiological manifestations, such as cancers, cardiovascular disease and amyloidogenic neurodegenerative disease, are corollary with PDI dysregulation and loss of proteostasis[70].

Structure of PDI

PDI consists of four highly conserved domains with an abb'xa' arrangement followed by a highly acidic C-terminal extension (Figure 10). The two catalytic (a & a') domains are separated by the non-catalytic (b & b') regions as well as the (x) loop linker[71]. Each catalytic domain consists of conserved Cys-Gly-His-Cys (CGHC) active site sequences that confer oxidoreductase activity through the cysteine residues. Each CGHC active site, when in the ER environment, has high reducing capabilities for disulfide groups, which lend to PDI's high oxidative potential[72]. The domain responsible for the chaperone function of PDI so as to inhibit protein aggregation and/or targeting of misfolded proteins for degradation remains unknown. It is hypothesized that this domain contains hydrophobic residues which allow for interaction with aggregated protein targets as the main substrate-binding site[73].

Function of PDI and the Unfolded Protein Response

The two major functions of PDI include 1) oxidoreductase activity, which can either oxidize, reduce, or isomerize disulfide bonds formed during post-translational folding, and 2) chaperone activity to block hydrophobic interactions of aggregated proteins and promote degradation of

terminally misfolded proteins or protein accumulation via the Unfolded Protein Response (UPR)[74].

1. The catalytic (a & a') domains operate independently of one another. According to Xu et. al, disruption of any one of the two CGHC active sites reduces oxidoreductase activity by 50%, where disruption of both active sites reduces oxidoreductase function altogether. The ability of PDI to alter disulfide bonds relies on the redox state of both PDI (influenced by electrochemical properties of the ER), as well as the target substrate[73].
2. The chaperone activity of PDI is conferred through the (b') domain. This site, rich in hydrophobic amino acids, is the primary substrate binding site which through hydrophobic interaction maintains a high-affinity interface with complementary regions of protein aggregates. Because the enzyme-substrate complex is maintained via hydrophobic van der Waals forces, the specificity of PDI is vast[73].

The Unfolded Protein Response (UPR) is the highly concerted process by which ER stress is monitored and ameliorated through several feedback pathways[75]. The UPR can discriminate between moderate and therefore abrogative ER stress generated through misfolded protein accumulation, as well as excessive or chronic ER stress which will prompt pro-apoptotic signal cascades[76]. ER stress sensors are tethered to the ER chaperone BiP. Under stressed conditions, the large concentration of misfolded proteins in the ER outcompete stress sensors for hydrophobic interaction with BiP, resulting in activation[77]. Three well characterized ER stress sensors which regulate UPR include 1) PKR-like endoplasmic reticulum kinase (PERK), 2) activating transcription factor 6 (ATF6), and 3) inositol-requiring kinase (IRE1). The

combinatorial effect of these sensors under moderate ER stress is ameliorative in that they inhibit translation, promote physical expansion of ER volume, and lead to transcriptional activation of ER chaperones such as PDI.

1. PERK: upon activation, PERK leads to phosphorylation of eukaryotic translation initiation factor 2α (eIF2α). Phosphorylation of eIF2α inhibits ubiquitous translation, yet confers selective translation of transcription factor ATF4 mRNA; AFT4 then translocates to the nucleus and initiates the production of PDI and other ER-localized chaperones[78].
2. ATF6: ATF6 is transported from the ER to the Golgi apparatus and cleaved to form ATF6 fragment (ATF6f) which then translocates to the nucleus and activates transcription of PDI and ER-associated degradative (ERAD) enzymes which subject terminally misfolded proteins to degradation[79].
3. IRE1: upon dimerization and phosphorylation, IRE1 activates and degrades mRNA with an ER signal sequence so as to prevent further accumulation of nascent proteins within the ER following translation. Furthermore, IRE1 splices the mRNA encoding transcription factor X-box binding protein 1 (XBP-1) which results in a frameshift mutation to the mRNA that allows for the production of a functional transcription factor. Newly synthesized XBP-1 moves to the nucleus and initiates the production of ERAD enzymes, and phospholipids. These effects enlarge the ER and allow for an increased quantity of ER chaperones[80,81].

Under chronic conditions of ER stress, as encountered through extensive accumulation of protein aggregates, the UPR stress signals convert from pro-protective to pro-apoptotic

cascades[82]. Prolonged activation of PERK leads to the production of C/EBP-homologous protein (CHOP), which subsequently inhibits the BCL-2 survival protein and simultaneously activates Bcl2-interacting mediator of cell death (BIM). These actions concertedly trigger the BAX- and BAK- dependent mitochondrial apoptotic caspase cascade[83]. Interestingly, CHOP has been demonstrated to contribute to conditions of oxidative stress by abstracting electrons from chaperones such as PDI and converting diatomic oxygen to hydrogen peroxide[80].

Redox Stress, PDI, and Neurodegenerative Disease

Reactive oxygen species (ROS) and reactive nitrogen species, in particular, have been reported to render PDI afunctional. Excess nitrosative stress can lead to a post-translationally S-nitrosylated form of PDI (SNO-PDI). The addition of the nitric monoxide to the thiol groups of each CGHC active site inhibit the oxidoreductase capabilities of the (a & a') domains; ultimately leading to an increase in misfolded proteins[84]. Uehara et al demonstrated a colocalization of SNO-PDI and α-SYN within LBs of post-mortem brains from PD patients. It should be noted, however, that the general chaperone mechanism of PDI is largely uncharacterized as is its vulnerability to redox stress. Because oxidative and nitrosative stress-mediated apoptosis is a prominent finding in cases of neurodegenerative disease and contributes to further protein aberrance, there appears to be a cyclical phenomenon by which protein misfolding contributes to ER stress and induces pro-apoptotic cascades that result in oxidative damage, thereby inhibiting chaperone molecules which in turn leads to further protein misfolding and ultimately progressive neuronal death.

This literature review lends insight into the etiology of PD, the molecular mechanism of PD pathogenesis, as well as the clinical insufficiencies that make PD the second-most common neurodegenerative disease worldwide. Furthermore, a review of DNA nanotechnology and molecular cell biology potentiate novel resolutions to the undeniable lack of quantitative diagnostics and target-specific therapeutic options for PD. This thesis contains a two-fold translational research study using 1) aptamer-based Dz systems to serve as an oligomeric α-SYN detection platform for early PD diagnosis, and 2) PDI to abrogate oligomeric α-SYN-mediated neuropathy as a potential gene therapy for PD.

CHAPTER TWO: APTAMER-BASED DEOXYRIBOZYME DETECTION OF OLIGOMERIC α-SYN

Materials and Methods

Aptamer Dot-Blot Detection of Oligomeric α-SYN

The Aptamer used, as reported by Ikeubkro et. al T-SO508, was purchased from GeneLink (Hawthorne, NY) biotinylated at the 5' end and purified via gel purification. The aptamer was reconstituted in Tris-HCl with EDTA pH 7.5 to a stock concentration of 200 µM. At the time of use, T-SO508 was brought to a working concentration of 5 µM in PBS-HCl pH 7.5 supplemented with 1 mM $MgCl_2$. The solution was aliquoted into thin-walled PCR tubes and incubated at 99°C for five minutes in a thermal cycler to denature and anneal the oligonucleotide. After five minutes the sample was allowed to cool to room temperature for approximately one hour in the sealed heat block.

Recombinant pre-fibrillar form (PFF)— oligomeric—and monomeric α-SYN, kindly provided by John's Hopkins, were diluted to 1 mg/ml in PBS and sonicated at 20Hz for one minute with 0.5-second pulses. After sonication, working samples of 1.0, 0.75, 0.5, and 0.25 mg/ml were prepped via serial dilution with PBS.

A PVDF membrane was activated in 100% Methanol for 30 seconds followed by a five-minute wash in water with shaking. A 2 µl aliquot of each monomeric and PFF α-SYN was blotted in the reaction zone and the membrane was allowed to dry for fifteen minutes. The membrane was then blocked in non-protein based blocking solution (LI-COR Biosciences Lincoln, NE) diluted to a 1X concentration with PBS plus 0.1% Tween-20 for one hour at room

temperature with rocking. After blocking the membrane was washed three times in 0.1% PBS-T wash buffer for ten minutes each. Annealed T-SO508 was added directly to each reaction zone and allowed to incubate in a humidified chamber at room temperature for approximately one hour. Using 0.05% PBS-T spiked with 1 mM $MgCl_2$, the membrane was washed three times for ten minutes each.

For colorimetric development, an Avidin-Biotin-HRP Complex (ABC) kit (Vector laboratories Burlingame, CA) was used. The ABC reaction mix was incubated with the membrane for no more than five minutes, followed by three fifteen minute washes with wash buffer and vigorous shaking. To develop, 2,2-diaminobenzidine substrate (DAB) (Vector laboratories Burlingame, CA) was added for immediate colorimetric development.
After confirmation of reactivity of the reported aptamer sequences to the α-SYN of use via dot blot, several sequences were selected and modified for deoxyribozyme (Dz) application (Table1).

Deoxyribozyme Detection Assays for Oligomeric α-SYN

Traditional BiDz, Tile Dz, and Aptamer Dz oligonucleotides were designed and provided (Integrated DNA Technologies Coralville, IA) kindly by D. Kolpashchikov of University of Central Florida, Department of Chemistry. Each sensor was purified through standard desalting (SD). The fluorogenic substrate (F_sub) (TriLink Bio Technologies, Inc. San Diego, CA) was purified via high-pressure liquid chromatography (HPLC) used at a working concentration of 200 nM per reaction. $BiDz_a$ and $BiDz_b$ were used at working concentrations of 2 nM and 50 nM, respectively. Aptamer Dz_a and Aptamer Dz_b were used at working concentrations of 2 nM and

50nM, respectively. In cases involving use of the tile-associated Dz sensor, 100 nM of each of the nine tile strands (T1-T9) were combined in reaction buffer and annealed by incubating in a 100°C water bath followed by gradual cooling overnight. The annealed tile was used at a working concentration of 2 nM per reaction mix. All assay reactions took place in Dz reaction buffer (50 mM HEPES, pH 7.4, 50 mM $MgCl_2$, 20 mM NaCl, 0.03% Triton X-100, and 1% DMSO) at a final volume of 60 µl.

Recombinant PFF was prepared as previously mentioned in working stocks of 100 µM and 10 µM. To determine the LOD of each class of sensor for α-SYN detection, a titration curve was used consisting of 1 nM, 10 nM, 20 nM, 50 nM, and 100 nM PFF. Analytes were incubated with each class of sensor for 1.5 and 18 hours at 30°C. Fluorescence values were obtained at an excitation/emission setting of 485/517 nm (Perkin-Elmer LS-55 spectrometer Waltham, MA).

Deoxyribozyme Specificity Assay to Oligomeric α-SYN

$BiDz_a$ and $BiDz_b$ were used at working concentrations of 2 nM and 50 nM, respectively. Aptamer Dz_a and Aptamer Dz_b were used at working concentrations of 2 nM and 50nM, respectively. The annealed Tile Dz was used at a working concentration of 2 nM per reaction mix. Dz_b was used at a concentration of 50 nM per reaction mix. Each of the three sets of sensor were incubated with 100 nM PFF, and 100 nM of monomeric α-SYN in parallel with a 26 µM thrombin negative control for 18 hours. Fluorescence values were obtained again at an excitation emission setting of 485/517 nm.

Results and Discussion

To explore the biologically compatible diagnostic potential for detecting oligomeric α-SYN, novel Dz sensors were utilized detect structure-specific α-SYN. The aims of using deoxyribozyme systems being: 1) to achieve lower limits of detection by manipulating the enzyme-kinetic properties of the Dz sensors and 2) to distinguish between pathological and native α-SYN structures. This will lay the foundation of a clinical neurological screening method that is standardized for early PD detection through use of a sensitive, specific, and quantitative diagnostic system with a quick and cost-effective turnaround time.

Colorimetric Dot Blot Revealed Aptamer Specificity to Oligomeric α-SYN

Aptamer sequences as communicated by Ikebukro et al were adapted for Dz design. Sequence T-SO508 was selected based on its reported affinity and specificity so as to ensure the reported sequences were compatible with the recombinant α-SYN of use. To test the preliminary specificity of T-SO508 before proceeding with Dz adaptation, a colorimetric dot blot was performed to probe for immobilized recombinant α-SYN (Figure 11). This system demonstrated selectivity to the oligomeric (PFF) species of α-SYN, without cross-reactivity to the monomeric species. However, 0.5 μg of immobilized oligomeric α-SYN (18 nM) was not significantly detectable even with the 4-fold amplification properties of the ABC system and considerably high concentration of aptamer probe as compared to Dz sensor concentrations.

Binary Dz, Tile Dz, and Aptamer Dz Limit of Detection of α-SYN

Raw (Figure 12) and adjusted (Figure 13) fluorescent values for each Dz system at 1.5 and 18 hours of incubation with α-SYN were compiled. Error bars are representative of the standard

deviation of each trial. It was evident that the 1.5-hour incubation produced no statistically significant means of detection, however an 18-hour incubation period did in fact produce a discernable signal sufficient for quantification. To determine the limit of detection of each system, the respective raw values were then plotted to generate a line of best fit (Figure 14**).** Using the formula $\frac{3.0\sigma - b}{m}$, the LOD for BiDz, Tile Dz, and Aptamer Dz were calculated to be 14.67 nM, 12.45 nM, and 7.95 nM, respectively. The Dz detection system demonstrates greater efficiency at detecting α-SYN by requiring nearly 100 times less sensor than traditional methods such as immobilized blotting and colorimetric development. The next phase of this work will consist of performing kinetic assays to determine the optimal incubation time between 1.5 and 18 hours, as it was previously demonstrated that 1.5 hours is insufficient required for significant signal accumulation. Thus, reducing the incubation time necessary to accurately perform the assay without compromising sensitivity.

Aptamer Dz System Preferentially Detects Oligomeric α-SYN

Of the three Dz systems evaluated for selectivity to oligomeric α-SYN over the monomeric species (Figure 15), the BiDz and Tile Dz showed no selectivity; in fact, they showed a ~25% preference to the monomeric species when compared to oligomeric. However, the Aptamer Dz system showed ~10% preference to the oligomeric species and will be further optimized to increase its specificity. None of the systems demonstrated reactivity to thrombin, which was used at a concentration of 26 μM, ten times the physiological plasma concentration.

There are two possible explanations as to why the BiDz and Tile Dz systems exhibited higher selectivity to the monomeric species:

1. The sequences referenced in the literature that were adapted and modified for this study were not originally selected against oligomeric α-SYN in the presence of a high-detergent buffer (such as that used for the Dz assays). Differences in salt and detergent concentrations can influence binding abilities of nucleotide sensors and as such may have caused a change in ligand affinity.
2. The BiDz and Tile Dz systems require "splitting" of the analyte-binding region, whereas the Aptamer Dz system relied on use of whole aptamer sequences adapted from Ikebukro et al. "Splitting" of oligonucleotide constructs for Dz adaptation can dramatically influence the analyte binding abilities; such that even a single nucleotide difference in location can affect the signal output.

The use of these Dz systems for protein detection is novel, and thus the data presented here illustrates proof-of-concept. Utilization of Dz diagnostics as presented in this work will lead to development of a proprietary oligonucleotide sequence for oligomeric α-SYN detection.

CHAPTER THREE: PDI Disruption of Oligomeric α-SYN

Materials and Methods

Recombinant PDI Deletion Construct Production

To purify recombinant full-length PDI as well as the library of deletion constructs, each pET28 bacterial expression vector (kindly provided by Dr. Kenneth Teter of University of Central Florida, Burnett School of Biomedical Sciences) was transformed into *E. coli* strain BL21 (New England Biolabs Ipswich, MA) . Overnight cultures were inoculated into Luria Muller broth with ampicillin selection (100 mg/ml) and grown to an optical density of 0.8 at 600 nm. Cultures were then induced at a final concentration of 2 mM IPTG at 37°C for four hours with shaking. Cells were pelleted at 6,000 rpm for twenty minutes at 4°C. Pellets were resuspended in extraction buffer (20 mM Tris-HCl pH 7.0, 300 mM NaCl). Cells were then lysed using lysozyme-based lysis buffer (extraction buffer, 0.1% Triton X-100, 1% sodium deoxycholate, 100 μg/ml lysozyme, and 0.1 μl/ml DNAse) followed by three, fifteen minute cycles of freezing (-80°C) and thawing (37°C). The lysate mixture was centrifuged at 12,000 RCF for thirty minutes at 4°C. The supernatant was collected and spiked with protease inhibitor cocktail (Roche Indianapolis, Indiana). Crude lysate was added to equilibrated talon resin slurry (Clontech Mountain View, CA) then agitated for thirty minutes at room temperature. The mixture was then centrifuged at 700 RCF for five minutes. After removal of the supernatant, the resin was resuspended with wash buffer (extraction buffer, 600 mM NaCl, and 0.1% Triton X-100) and incubated at room temperature for fifteen minutes with agitation. The solution was centrifuged at 700 RCF for five minutes and supernatant collected; this process was repeated twice. Extraction buffer was used to

resuspend the washed resin and the solution was loaded into a gravity flow column. To elute the His-tagged proteins, a gradient of imidazole (10 mM, 20 mM, and 40 mM) in extraction extraction buffer was used. There were four rounds of elution per imidazole concentration in 500 µl increments. Fractions were then denatured, electrophoresed via 10% SDS-PAGE, and visualized using a Coomassie brilliant blue staining (1.0 g coomassie brilliant blue, 50% [v/v] methanol, and 10% [v/v] glacial acetic acid) followed by destaining (40% [v/v] Methanol and 10% [v/v] glacial acetic acid).

pcDNA3.1 Cloning

Primers were designed to contain 5' *BamHI* and 3' *EcoRI* cut sites for downstream digestion-ligation reactions, along with a 5' 6X Histidine tag (Table 2). PDI cDNA and deletion constructs were amplified using a standard amfiSure Taq polymerase master mix (GenDEPOT Barker, TX) using a 5°C gradient PCR for optimal purity. The cDNA was purified via UV transillumination and Zymoclean gel DNA recovery kit (Zymo research group Irvine, CA). cDNA and pcDNA3.1 vector were double-digested using *BamHI* and *EcoRI* restriction endonucleases (Fermentas Thermo Scientific Grand Island, NY) at 37°C overnight. Following another round of gel extraction and purification, digested vector and insert were ligated overnight using T4 DNA Ligase (New England Biolabs Ipswich, MA) at 4°C. Ligation reactions were subsequently transformed into calcium chloride competent DH5α E. coli (New England Biolabs Ipswich, MA) using a heat shock regimen (4ºC for thirty minutes, 42°C for fifty seconds, 4°C for three minutes) followed by a one hour recovery stage in Super Optimal Broth with Catabolic repression (SOC) at 37°C before being plated on LB agar plates with ampicillin (100 mg/ml). Clones were pre-

screened via colony PCR method to determine potential positive clones (Promega Madison, WI). Sanger sequencing was used to determine removal of N-terminal ER retention sequence (GENEWIZ South Plainfield, NJ). Plasmid DNA was then isolated in bulk via GeneJET Plasmid Miniprep kit (Thermo Fisher Scientific Waltham, MA).

Cell Culture

All cellular studies were performed in Human Embryonic Kidney 293T (HEK 293T) immortalized cell line in Dulbecco's Modified Eagle's Media with 10% fetal bovine serum (Atlanta Biologicals Flowery Branch, GA). Transfections were prepared by seeding cells such that they reached 50% confluency at the day of transfection. Transfections were performed using X-fect transfection reagent (Clontech Mountain View, CA) with a four-hour incubation period in serum-free media followed by a complete media change.

PDI Overexpression

Cells were transfected with 2.5 µg of recombinant pcDNA3.1 PDI or 2.5 µg of pcDNA3.1 empty vector and allowed to incubate for a forty-eight hour post transfection period before harvesting via trituration in 1X PBS with protease inhibitor cocktail.

α-SYN Overexpression and Aggregation Induction for Biochemical Assay

Cells were transfected with 2.5 µg pAAV-IRES-hrGFP-wt SNCA, 2.5 µg pAAV-IRES-hrGFP-S42Y SNCA, and 2.5 µg pAAV-IRES-hrGFP empty vector (designed by the lab of Dr. Yoon-Seong Kim of University of Central Florida, Burnett School of Biomedical Sciences). Cells were allowed to incubate for a forty-eight hour post-transfection period with routine media changes.

Approximately four hours prior to collection, cell media was spiked with 500 nM MG132. Cells were rinsed with PBS and collected by trituration in PBS spiked with protease inhibitor cocktail.

Split Protein Complementation Assay

Cells were triple transfected with 250 ng syn-hGLuc1 (SL1) and 250 ng syn-hGLuc (SL2) (kindly provided by Dr. Pamela McLean of Massachusetts General Hospital, Boston, MA) and either 500 ng of pcDNA3.1 vehicle or pcDNA3.1 PDI overexpression vectors in HEK 293T cells. Forty-eight hours post-transfection, cells were rinsed with 100 µl of PBS, and lysed by adding 50 µl of Cell Lysis Buffer (Pierce Biotechnology Rockford, IL) in each well and incubating for thirty minutes at room temperature with orbital shaking. Crude lysates were collected and spun down at 16,000 RCF for five minutes at room temperature. Supernatants were collected and protein concentration determined as previously mentioned. 20 µg normalized samples were loaded into a black-bottom 96 well plate and 50 µl of coelenterazine working solution (Pierce Biotechnology Rockford, IL) was added to each well before luminometry via EnVision Multilabel Reader (Perkin Elmer Waltham, MA).

Immunoblotting

Reducing SDS-PAGE

Cells were harvested in PBS and lysed using radioimmunoprecipitation buffer (RIPA) and spun-down at 14,000 RCF for fifteen minutes at 4°C. Supernatants were extracted, concentration determined via detergent compatible Lowry assay (BioRad Hercules, CA) and normalized. Samples were denatured by boiling for five minutes in 4X reducing Laemmli buffer (40% [v/v]

glycerol, 240 mM Tris-HCl pH 6.8, 8% SDS [w/v], 0.04% bromophenol blue [w/v], and 5% [v/v] beta-mercaptoethanol), followed by immediate cooling on ice and electrophoresed on a denaturing polyacrylamide gel. Following a Western transfer onto a 0.18 μm nitrocellulose membrane (BioRad Hercules, CA), the membrane was blocked in 5% milk in 0.1% TBS-T. Primary antibodies and dilutions included: primary anti-His Tag antibody (Santa Cruz Biotechnology Dallas, TX) at a 1:1,000 dilution and Syn-1 antibody (BD biosciences San Jose, CA) at a 1:500 dilution. Secondary antibodies and dilutions consisted of anti-mouse secondary antibody conjugated to HRP at a 1:5,000 dilution (Thermo Fisher Grand Island, NY). All primary antibody incubations occurred at 4°C overnight, while all secondary antibody incubations occurred at room temperature for one hour. Blots were developed using enhanced chemiluminescent reactions (ECL).

Non-Reducing SDS-PAGE

Cells were washed with PBS, collected by trituration, and resuspended in PBS-T spiked with EDTA-free protease inhibitor cocktail. To lyse the cells, the suspension was sonicated at 40 Hz two times for fifteen seconds each. Lysates were then spun down at 20,000 RCF for twenty minutes at 4°C and protein concentration determined via detergent compatible Lowry assay. After normalization, the samples were treated with 4X sample buffer, free of beta-mercaptoethanol (1X PBS, 10% FBS, 1% BSA, 0.1% bromophenol blue) and denatured at 99°C for five minutes followed by cooling on ice. Samples were loaded onto a 5% SDS-PAGE gel with a 4% stacking gel and electrophoresed at 100 V for two hours. After electrophoresis, the gel was transferred to a 0.18 μm nitrocellulose membrane with the stacking gel intact and proteins

were transferred for two hours at 90 V at room temperature. After transfer, the membrane was fixed with 0.4% paraformaldehyde (PFA) for thirty minutes at room temperature, followed by a brief wash in 0.1% TBS-T and blocking with 5% skim milk. The membrane was incubated with primary Syn-1 antibody (BD biosciences San Jose, CA) at a 1:500 dilution per 20 µg of loaded protein overnight at 4°C with rocking. Following three, ten minute washes, the membrane was incubated with anti-mouse secondary antibody conjugated to HRP at a 1:5,000 dilution (Thermo Fisher Grand Island, NY) for one hour at room temperature with rocking. After another round of washing, detection proceeded through ECL reaction.

Results and Discussion

Full Length PDI and Deletion Constructs Purified for Downstream in vitro Assay

Full-length PDI, as well as the *abb'x* and *bb'x* deletion constructs (Figure 16), were successfully transformed and purified from BL21 (Figure 17). Future work will consist of purification of several other deletion constructs (bb'xa'x and b'xa'c) as well as optimization of a Thioflavin T (ThT) assay.

ThT is a fluorogenic compound that upon interaction with amyloid fibers (i.e. oligomeric α-SYN) becomes fluorescent and can be quantified at an excitation/emission wavelength of 450/482 nm, respectively. Through this technique, purified full-length and deletion constructs will be analyzed to ascertain which domain(s) are solely responsible for PDI's chaperone activity and at what optimal ratio it functions to disrupt synucleinopathies in vitro. Furthermore, time

point optimization will occur to determine the range at which PDI, and appropriate deletion constructs, are able to function as a disaggregase to reverse preexisting α-SYN oligomers.

PDI Inhibits α-SYN Aggregation in Live Cells as Reported by Complementation Assay

Full-length PDI and the *abb'x* and *bb'x* deletion constructs were successfully cloned into the pcDNA3.1 mammalian expression system (Figure 18). The N-terminal ER retention sequence was successfully removed so as to target PDI expression to the cytosol; This deletion was then confirmed by Sanger sequencing and qualitatively analyzed via agarose gel electrophoresis (Figure 19). Western blot analysis of 293T lysates transfected with pcDNA3.1 PDI expression vector demonstrated successful translation under the CMV promoter (Figure 20).

To monitor the preventative effects PDI has on α-SYN aggregation in live cells, a previously reported protein-fragment complementation assay (PCA) as communicated from McLean et al was used[85]. This system relies on two separate overexpression plasmids, each bearing a complete α-SYN expression sequence, tethered to either the N-sequence (AA1-93) or C-sequence (AA94-185) of a Gaussia luciferase (Gluc) gene (Figure 21). Upon aggregation of the α-SYN molecules, the N- and C-fragments are brought within close proximity to each other to create a functional Gluc protein, which can be quantified via traditional luminometry upon addition of the substrate coelenterazine. Quantification of PDI treatment in live cells using the split-complementation aggregation reporter assay revealed a ~25% decrease in luciferase signal, suggesting inhibition of α-SYN oligomerization in live cells (Figure 22). To support this analysis, a western blot of lysate samples revealed a controlled plasmid transfection paradigm (Figure 23).

Using a non-reducing SDS-PAGE, a live cell aggregation assay has been optimized wherein supramolecular oligomers of native, untagged α-SYN can be resolved via low percentage acrylamide gel to reveal "smearing" upstream of the 14 kDa monomeric α-SYN band. A lysate containing hyper-aggregative S42Y mutated α-SYN was used as a positive control, while non-transfected 293T was used to demonstrate strictly monomeric α-SYN as it would appear using this electrophoretic technique (Figure 24). With this technique, quantification of the smearing intensity both with and without PDI treatment will offer a biochemical assaying technique. This will be used to corroborate the split-complementation assay and evaluate potential differences in PDI treatment using untagged α-SYN (which may exhibit a different biochemical profile as compared to α-SYN that is tagged to the 20 kDa Gaussia luciferase protein).

Future work will consist of repeating the split complementation luciferase assay using the deletion constructs to determine which domain is responsible for the chaperone activity and henceforth explored as a gene therapy. A tetracycline-inducible PDI expression cell line will be generated so as to characterize the extent of PDI's reversal abilities in live cells. Furthermore, a modified non-reducing SDS-PAGE has been optimized and will be used to quantify oligomeric α-SYN species and PDI-mediated abrogation. Concomitantly, a live cell amyloid staining procedure coupled to flow cytometric analysis will be optimized to corroborate the findings presented by the split-complementation assay and SDS-PAGE biochemical assay.

CHAPTER FOUR: FIGURES AND TABLES

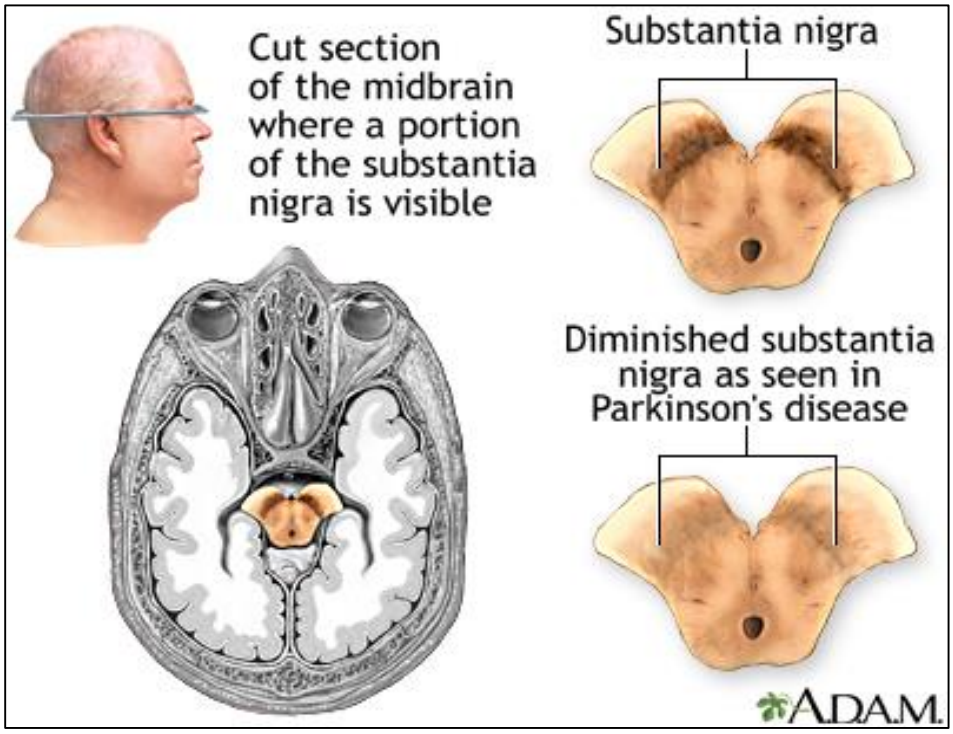

http://www.umm.edu/health/medical/reports/articles/parkinsons-disease

Figure 1: Anatomical Distinctions Between the Substantia Nigra Pars Compacta in Patients with Parkinson's Disease and Healthy Control

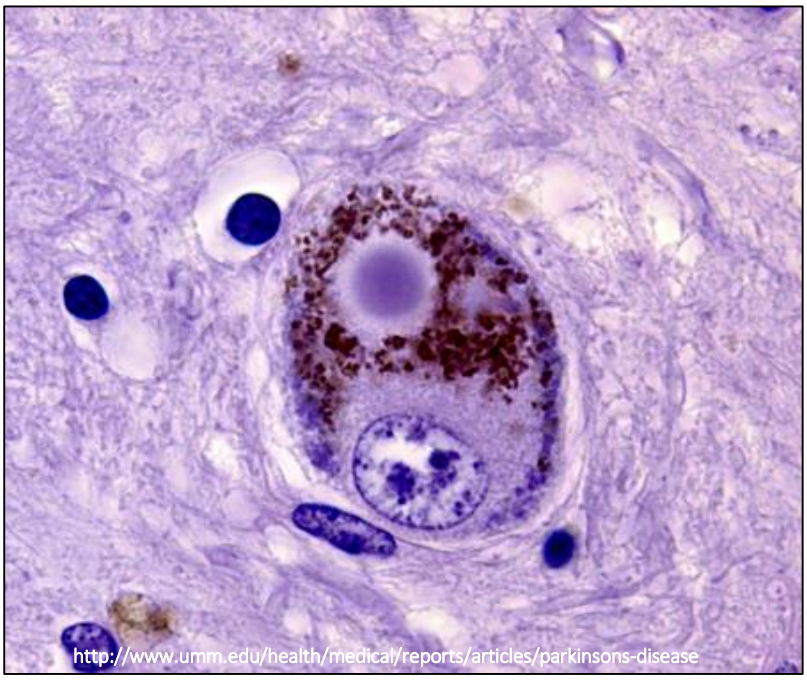

Figure 2: Histological Profile of Intraneuronal Lewy Body

Cross-sectional tissue stain from the Substantia Nigra illustrating Lewy Body. Melanin crystals appear as brown spots within the LB.

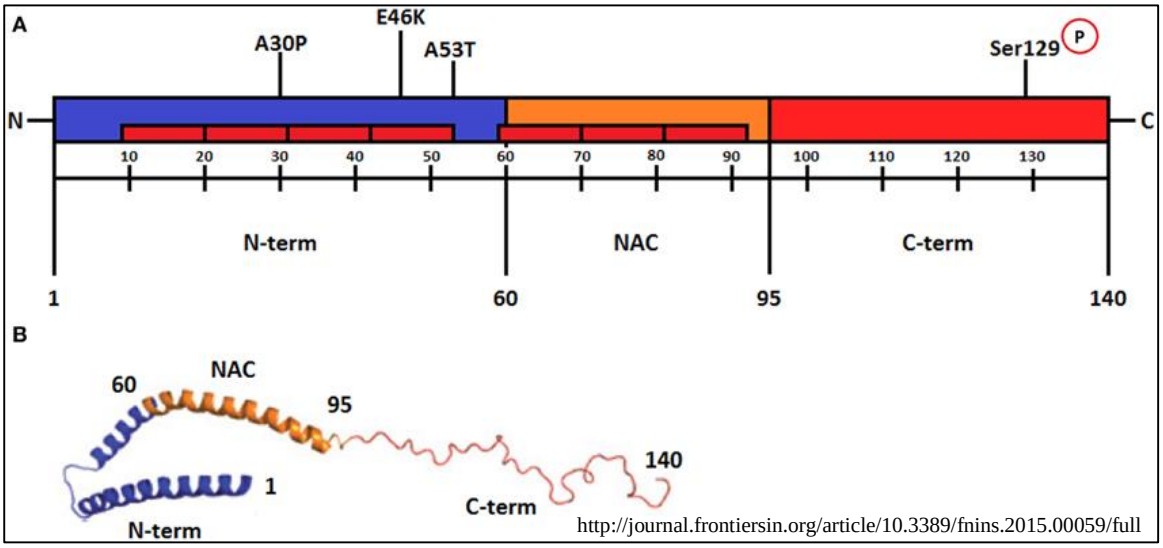

Figure 3: Structural Representation and Biochemical Hotspots of alpha-Synuclein

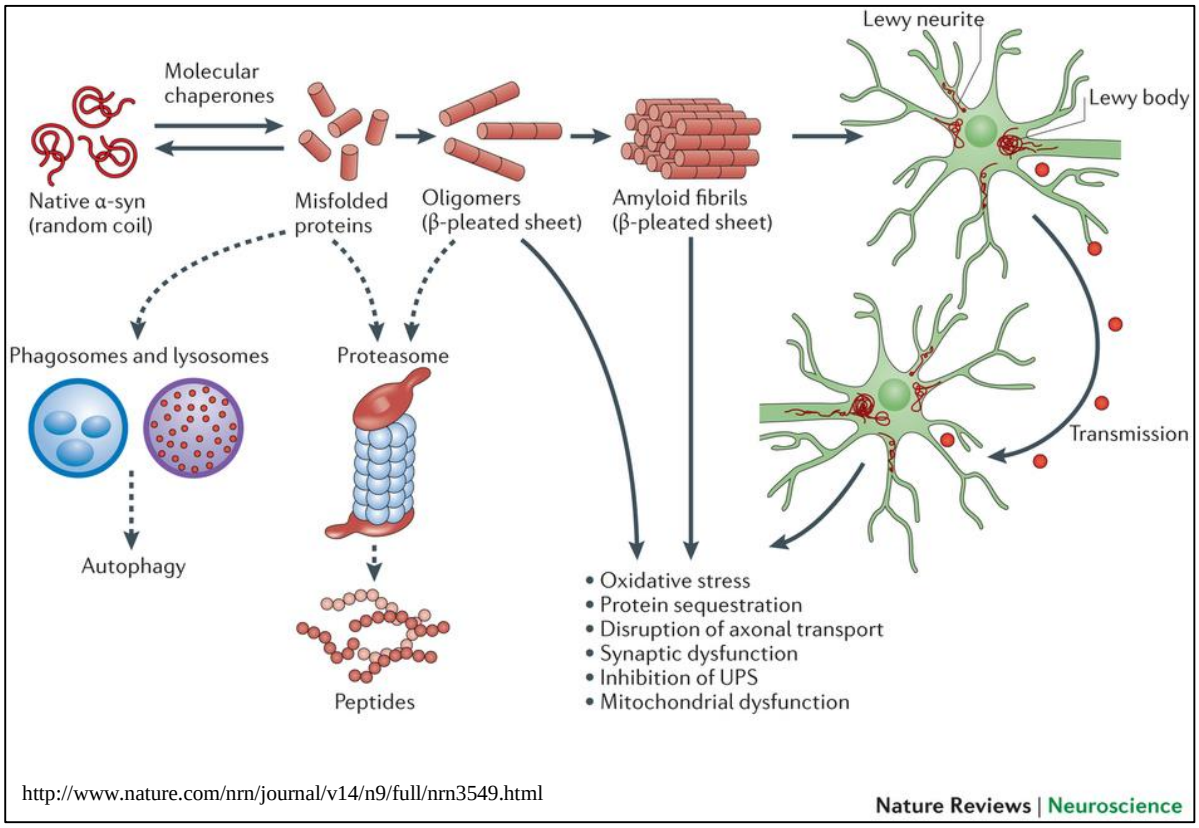

Figure 4: alpha-Synuclein Aggregation Cascade

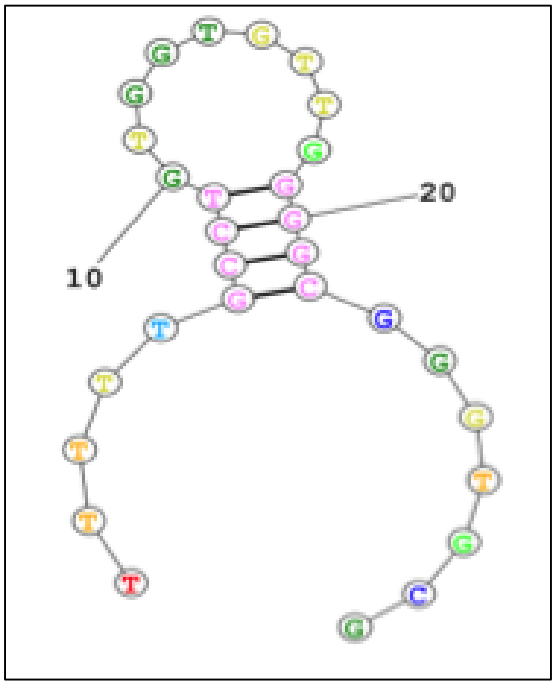

Figure 5: ssDNA Aptamer Secondary Structure

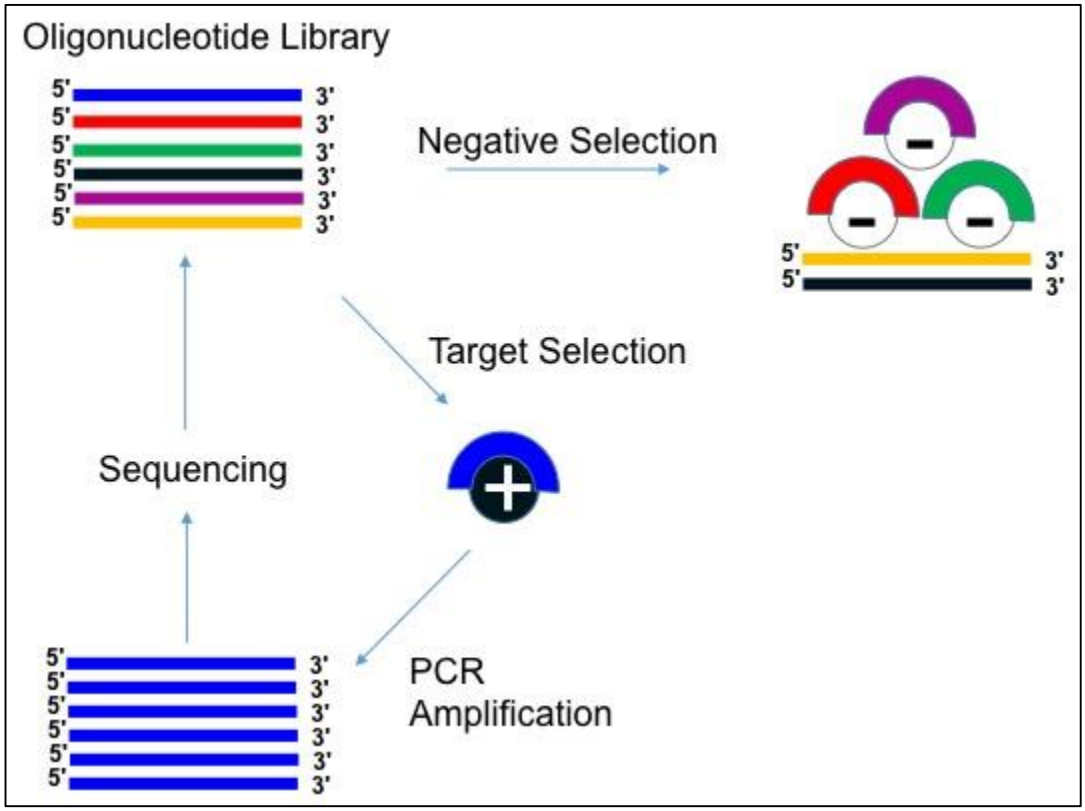

Figure 6: Tuerk and Gold SELEX Method for Aptamer Selection and Enrichment

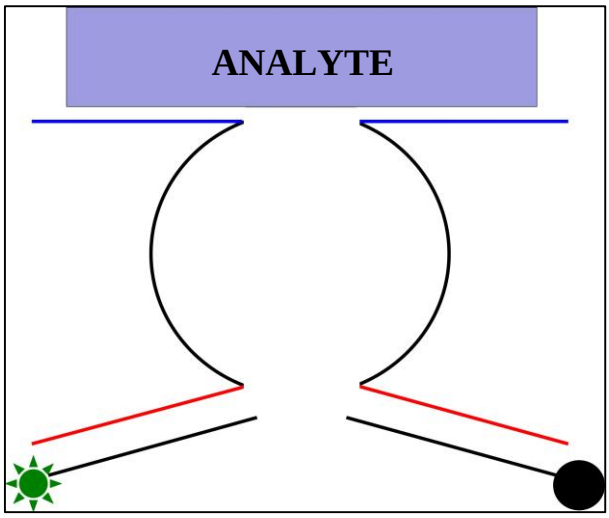

Figure 7: Binary Deoxyribozyme Schematic

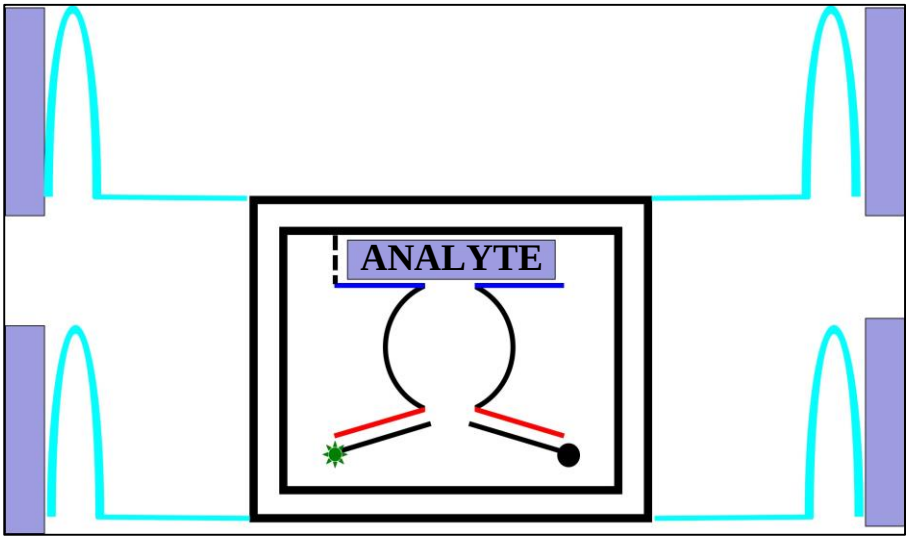

Figure 8: Tile Deoxyribozyme Platform Schematic

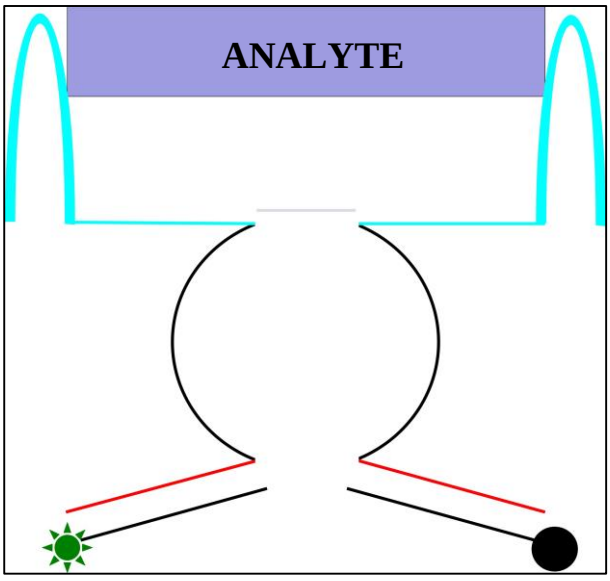

Figure 9: Aptamer Deoxyribozyme Schematic

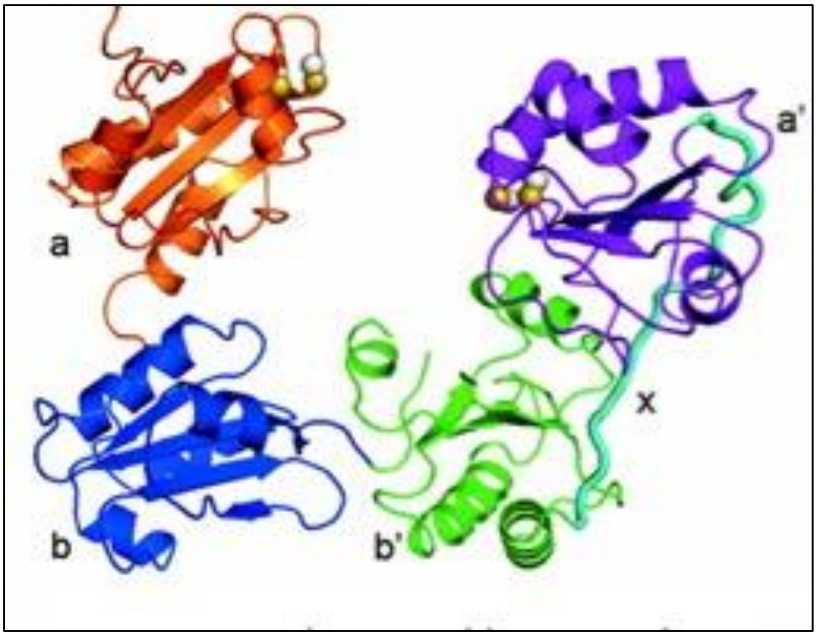

Figure 10: Ribbon Model of Protein Disulfide Isomerase

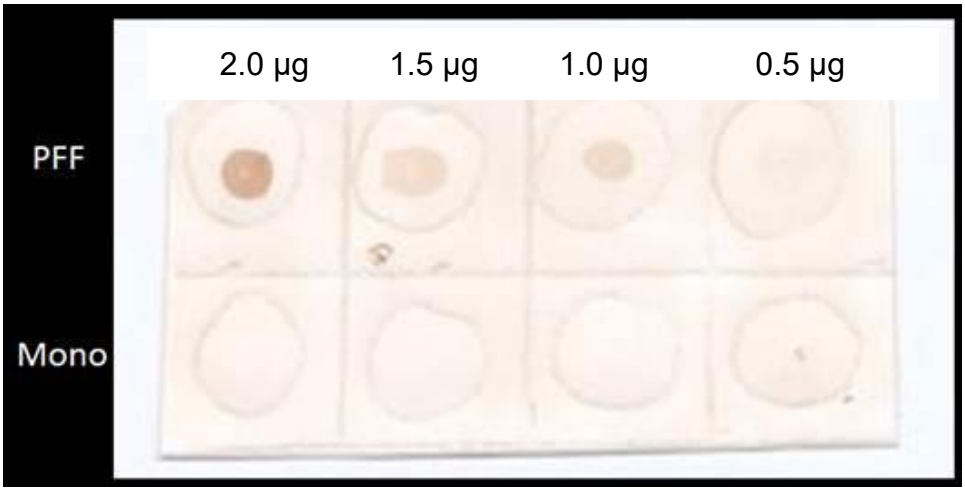

Figure 11: Dot Blot Confirmation of Aptamer Specificity Before Deoxyribozyme Adaptation

Table 1: Oligonucleotides Used for Deoxyribozyme Generation

Name	Sequence 5'→ 3'[a,b,c,d,e]	Purification [b]
F_sub-1	CGGT ACA TTG TAG AAG TT AAG GTT^{FAM} TCC TCg uCC CTG GGC A-BHQ1	HPLC
F_sub	AAG GTT^{FAM} TCC TCg uCCC TGG GCA-BHQ1	HPLC
Hilt_T-SO504	CGGT ACA TTG TAG AAG TT CAG GGG TGG GCA AAG GGC GGT GGT G	SD
T-SO504 complement	CAC CAC CGC CCT TTG CCC ACC CCT G	SD
Dza (Syn)_RT_T-SO504	**CAG GGG TGG GC** /iSp9/A CAA CGA GAGGAAAC	SD
Dzb (Syn)_RT_T-SO504	CCA GGG A GG CTA GCT /iSp9/**GGG CGG TGG TG**	SD
T1	CTC TAC TGA CGT GCC G *TTT* CGTCGATACGATGCA GTACTGTCGCAT *TTT* CTC TAC TGA CGT GCC G	SD
T2	CTC TAC TGA CGT GCC G *TTT* AGCTGATCACACT AGATTCTG TAG TGCATCGTATCGACG *TTT* CTC TAC TGA CGT GCC G	SD
T3	CTC TAC TGA CGT GCC G *TTT* ATGCGACAGTAC CCG ATC GTC ATG AGC ACC TAA CTT TTG GCC ATCA CCC CAC CAA CA AGC	SD
T4	CTC TAC TGA CGT GCC G *TTT* GTAACGACCGAT G AGTGTGATCAGCT *TTT* CTC TAC TGA CGT GCC G	SD
T6	CTC TAC TGA CGT GCC G *TTT*AGTTAGGTCTCA GCATCATCGAGCCTGA *TTT* CTC TAC TGA CGT GCC G	SD
T7	G TAT TCG GTA TTA GAC CCA GTT T CCCAG *TTT* AGACCGTGAGCATTGA CAACTGGATC GC ATCGGTCGTTAC *TTT* CTC TAC TGA CGT GCC G	SD
T8	CTC TAC TGA CGT GCC G *TTT* TCAGGCTCGATGATGC AGTCTCAGGT CACTGAACTGGTAGCGTACC *TTT* CTC TAC TGA CGT GCC G	SD
T5 (Dza_alpha syn)	**CAGGGGTGGGC** /iSp9/A CAA CGA GAGGAAAC TTT CAG AAT CTC GAT CCA GTT GAC CTG AGA CTT GAC GAT CGG CAT	SD
Hook	AA CTT CTA CAA TGT ACCG *TTTTT* CGG CAC GTC AGT AGA G	SD
Dza_ 508 (full)	**GCCTGTGGTGTTGGGGCGGGTGCG** /iSp18/*A CAA CGA* GAGGAAAC	SD
Dzb_508 (full)	CCA GGG A *GG CTA GCT* /iSp18/ **GCCTGTGGTGTTGGGGCGGGTGCG**	SD

[a]BHQ-1 – Black Hole Quencher1 [b]SD, standard desalting [c]iSp9, internal triethylene glycol spacer (IDT)
[d]Ribonucleotides are in lower case [e]oligo thymidine linkers are in italics.

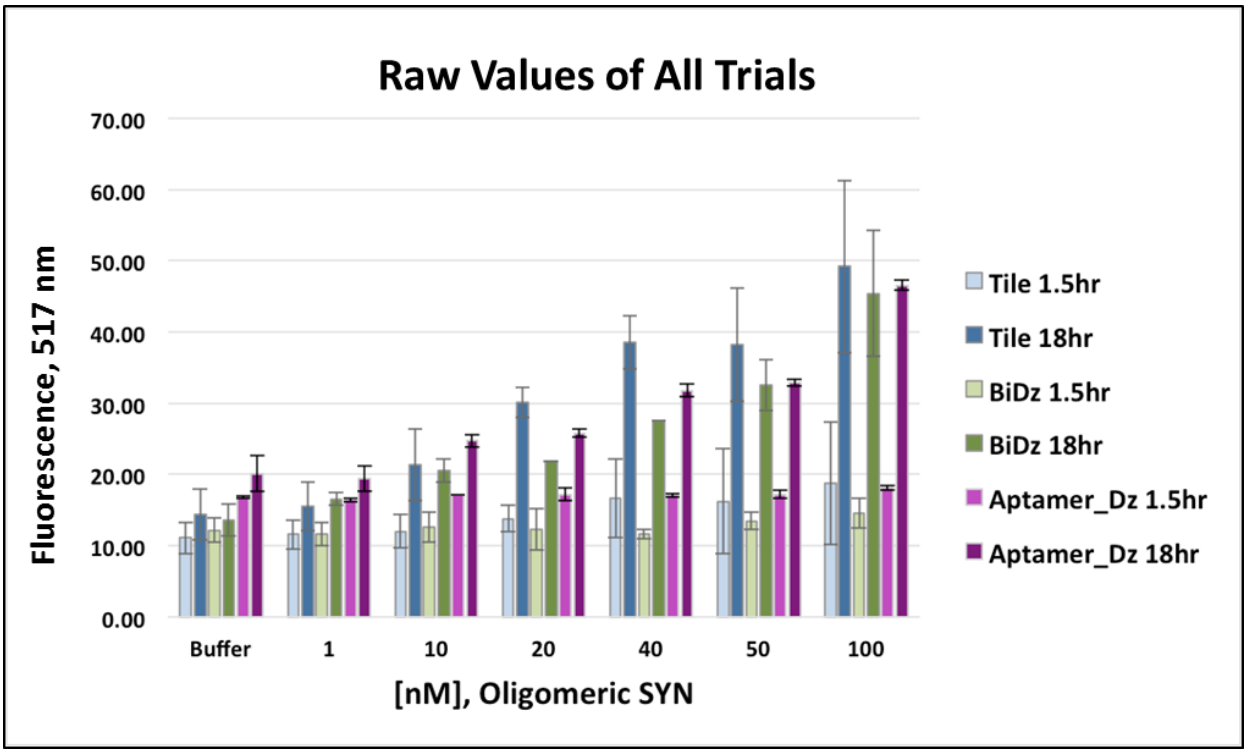

Figure 12: Average Raw Fluorescence Values for All Trials

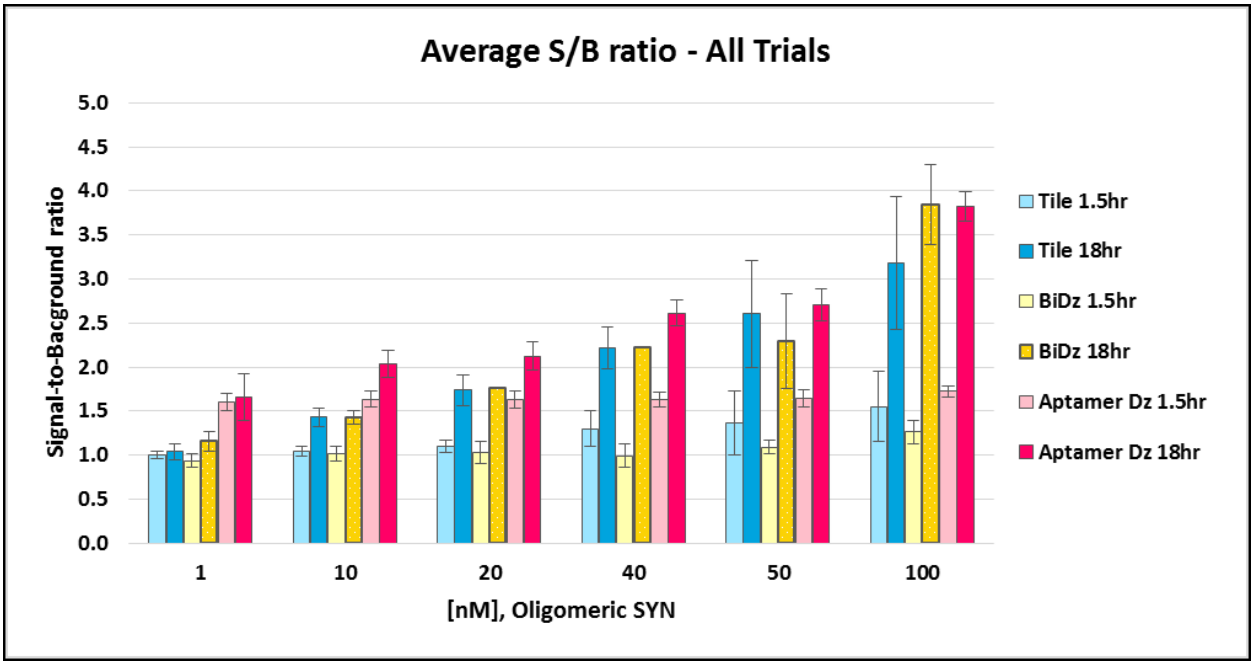

Figure 13: Average Signal-to-Background Ratios of Deoxyribozyme Activity

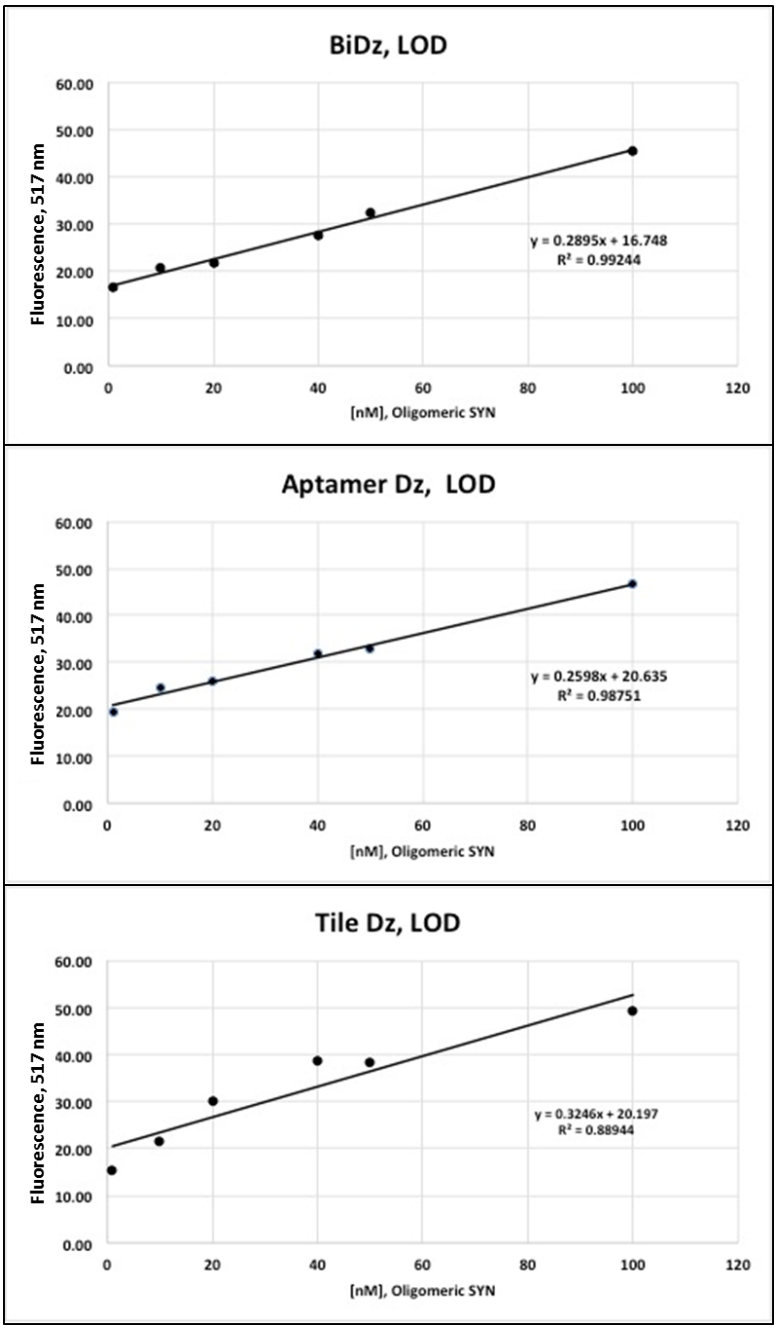

Figure 14: Limit of Detection Curves for the Deoxyribozyme Platforms after 18-Hour Incubation

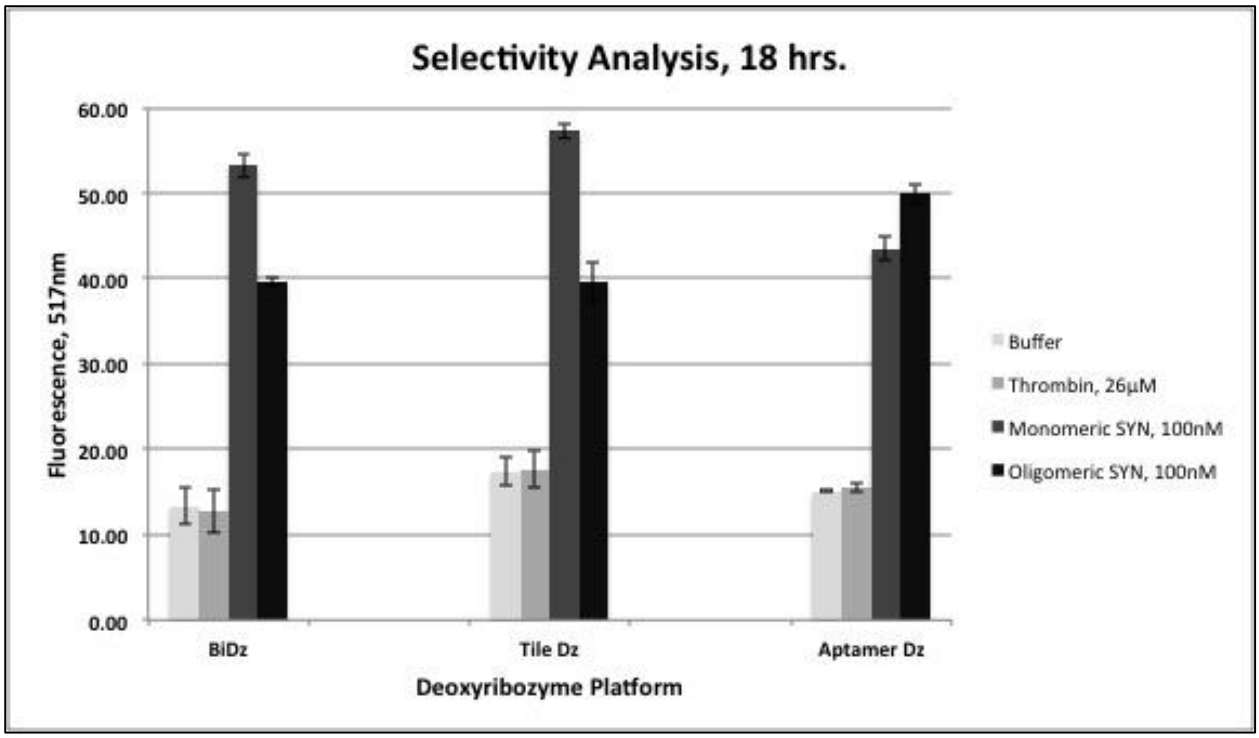

Figure 15: Selectivity Analysis for Each Deoxyribozyme Platform After 18-Hour Incubation

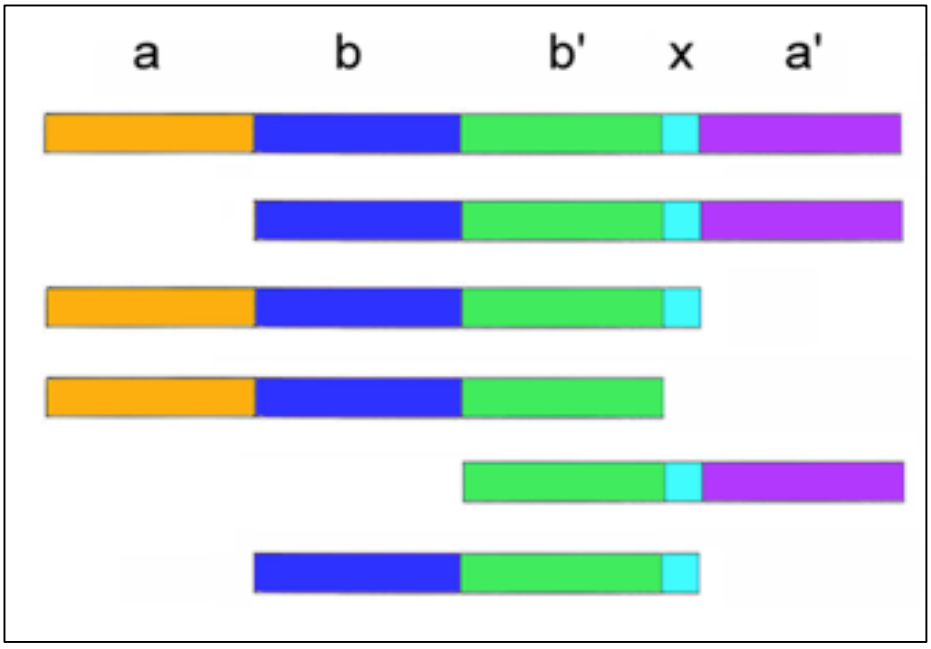

Figure 16: Protein Disulfide Isomerase Deletion Construct Library

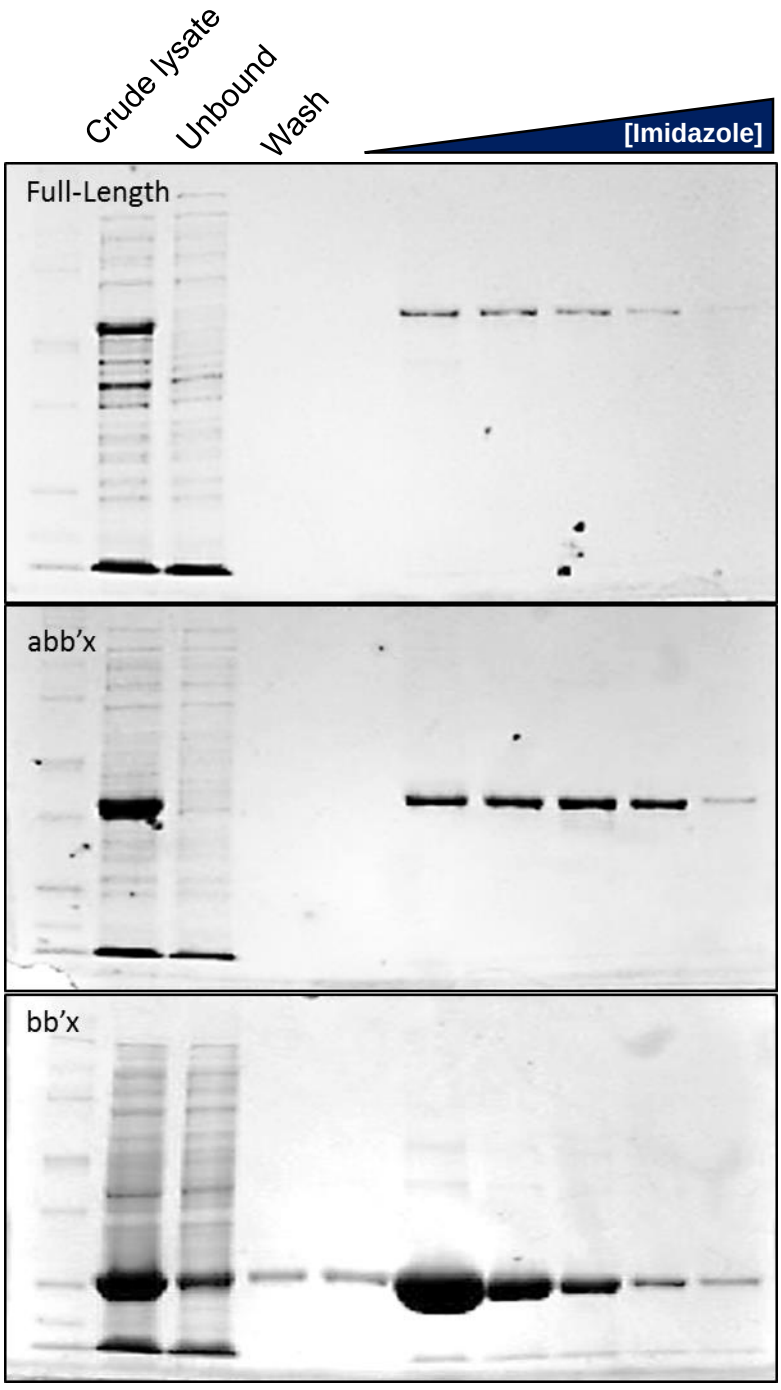

Figure 17:Protein Disulfide Isomerase Deletion Construct Purification Scheme

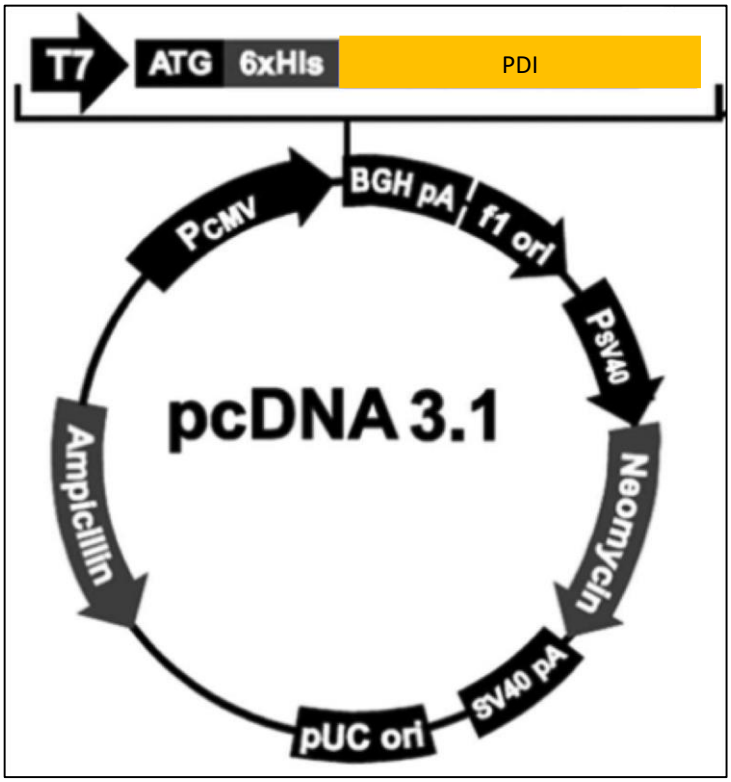

Figure 18: Cloned pcDNA3.1 PDI Mammalian Overexpression Vector

Table 2: DNA Primers Used for the Cloning PDI and Appropriate Deletion Constructs

Primer Name	Sequence (5'→3')	T_m	ΔG°
Universal Forward	TTATGCGGATCCATGCATCACCATCACCACCATA	64.5	-1.65
Full-length Reverse	AATACGGAATTCTTACAGTTCATCTTTCACAGCTTTCT	58.6	-1.28
x Reverse	AATACGGAATTCTTAAGGCTGCTTGTCCCAGT	62.5	-0.97

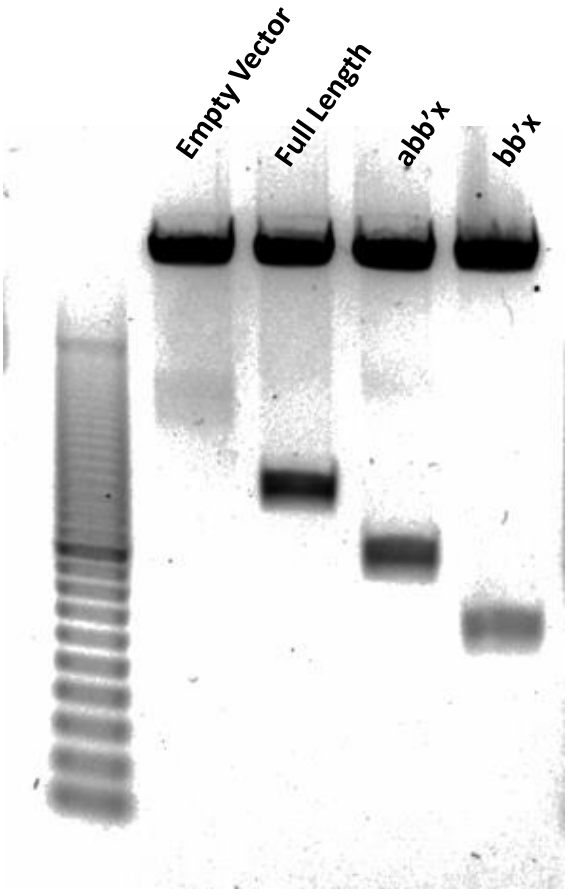

Figure 19: Agarose Gel of PDI Deletion Constructs Subcloned to pcDNA3.1

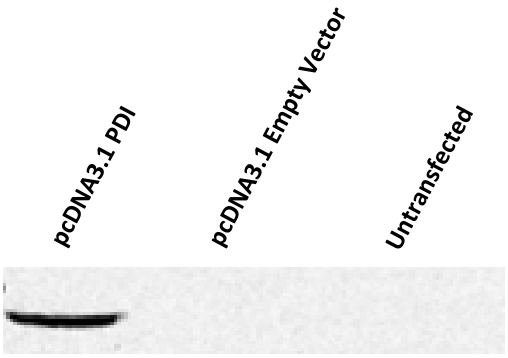

Figure 20: Western Blot Confirmation of PDI Expression in pcDNA3.1System

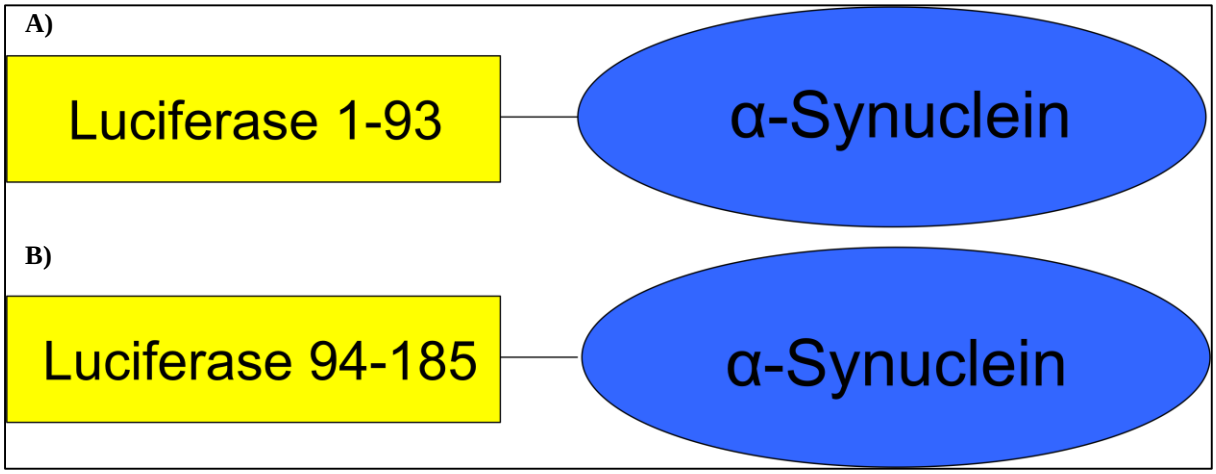

Figure 21: Split Complementation Luciferase Aggregation Reporter Schematic

Each construct (A and B) are expressed from separate co-transfected overexpression plasmids. As α-SYN aggregates, the tethered luciferase fragments are brought within close proximity of each other to create a functional luciferase gene. Lack of aggregation or transfection of only one plasmid will not produce a functional luciferase protein

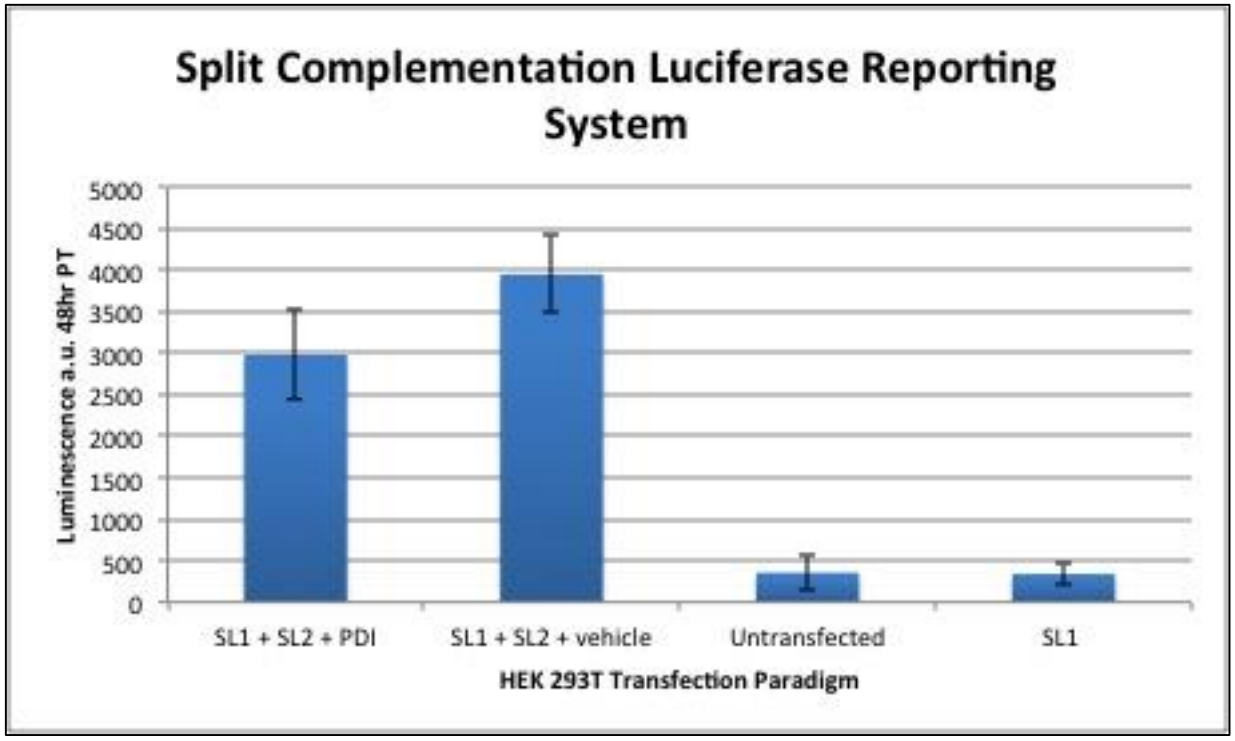

Figure 22: Luciferase Values After PDI Coexpression with Luciferase Reporting System

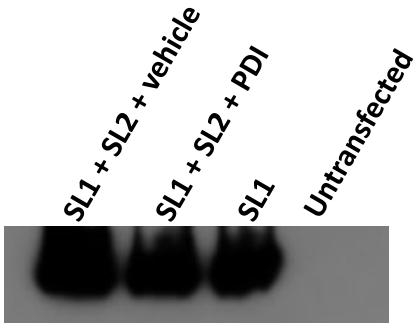

Figure 23: Western Blot Control of Split Complementation Triple Transfection

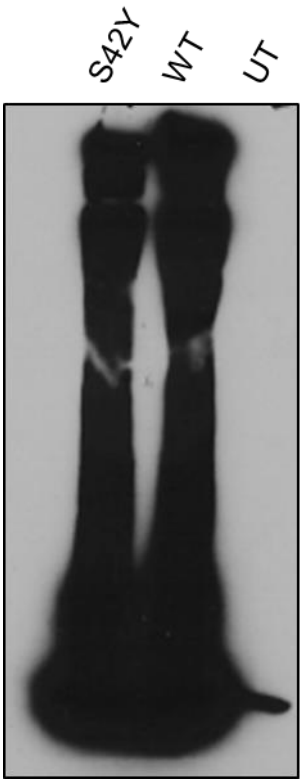

Figure 24: Modified SDS-PAGE for Live Cell Aggregation Monitoring

REFERENCES

1 de Lau, L. M. & Breteler, M. M. Epidemiology of Parkinson's disease. *Lancet Neurol* **5**, 525-535, doi:10.1016/S1474-4422(06)70471-9 (2006).

2 Jankovic, J. Parkinson's disease: clinical features and diagnosis. *J Neurol Neurosurg Psychiatry* **79**, 368-376, doi:10.1136/jnnp.2007.131045 (2008).

3 Schrag, A., Ben-Shlomo, Y. & Quinn, N. How valid is the clinical diagnosis of Parkinson's disease in the community? *J Neurol Neurosurg Psychiatry* **73**, 529-534 (2002).

4 Yaka, E. *et al.* Biological markers in cerebrospinal fluid (CSF) and evaluation of in vitro effect of CSF on PC12 cell line viability in Alzheimer's disease. *Cell Biochem Funct* **27**, 395-401, doi:10.1002/cbf.1588 (2009).

5 Massano, J. & Bhatia, K. P. Clinical approach to Parkinson's disease: features, diagnosis, and principles of management. *Cold Spring Harb Perspect Med* **2**, a008870, doi:10.1101/cshperspect.a008870 (2012).

6 Lees, A. J., Hardy, J. & Revesz, T. Parkinson's disease. *Lancet* **373**, 2055-2066, doi:10.1016/S0140-6736(09)60492-X (2009).

7 Nussbaum, R. L. & Ellis, C. E. Alzheimer's disease and Parkinson's disease. *N Engl J Med* **348**, 1356-1364, doi:10.1056/NEJM2003ra020003 (2003).

8 Deuschl, G., Bain, P. & Brin, M. Consensus statement of the Movement Disorder Society on Tremor. Ad Hoc Scientific Committee. *Movement disorders : official journal of the Movement Disorder Society* **13 Suppl 3**, 2-23 (1998).

9 Rodriguez-Oroz, M. C. *et al.* Initial clinical manifestations of Parkinson's disease: features and pathophysiological mechanisms. *The Lancet. Neurology* **8**, 1128-1139, doi:10.1016/S1474-4422(09)70293-5 (2009).

10 Sethi, K. Levodopa unresponsive symptoms in Parkinson disease. *Movement disorders : official journal of the Movement Disorder Society* **23 Suppl 3**, S521-533, doi:10.1002/mds.22049 (2008).

11 Lim, S. Y., Fox, S. H. & Lang, A. E. Overview of the extranigral aspects of Parkinson disease. *Arch Neurol* **66**, 167-172, doi:10.1001/archneurol.2008.561 (2009).

12 Hughes, A. J., Daniel, S. E., Kilford, L. & Lees, A. J. Accuracy of clinical diagnosis of idiopathic Parkinson's disease: a clinico-pathological study of 100 cases. *J Neurol Neurosurg Psychiatry* **55**, 181-184 (1992).

13 Newman, E. J. *et al.* Accuracy of Parkinson's disease diagnosis in 610 general practice patients in the West of Scotland. *Mov Disord* **24**, 2379-2385, doi:10.1002/mds.22829 (2009).

14 Huang, W. S. *et al.* Crossover study of (99m)Tc-TRODAT-1 SPECT and (18)F-FDOPA PET in Parkinson's disease patients. *J Nucl Med* **44**, 999-1005 (2003).

15 Eller, M. & Williams, D. R. Biological fluid biomarkers in neurodegenerative parkinsonism. *Nat Rev Neurol* **5**, 561-570, doi:10.1038/nrneurol.2009.135 (2009).

16 Jankovic, J. & Aguilar, L. G. Current approaches to the treatment of Parkinson's disease. *Neuropsychiatr Dis Treat* **4**, 743-757 (2008).

17 Cummings, J. L. *et al.* The role of dopaminergic imaging in patients with symptoms of dopaminergic system neurodegeneration. *Brain* **134**, 3146-3166, doi:10.1093/brain/awr177 (2011).

18 Lucking, C. B. *et al.* Association between early-onset Parkinson's disease and mutations in the parkin gene. *N Engl J Med* **342**, 1560-1567, doi:10.1056/NEJM200005253422103 (2000).

19 Ruottinen, H. M. & Rinne, U. K. COMT inhibition in the treatment of Parkinson's disease. *J Neurol* **245**, P25-34 (1998).

20 Lees, A. J., Ratziu, V., Tolosa, E. & Oertel, W. H. Safety and tolerability of adjunctive tolcapone treatment in patients with early Parkinson's disease. *J Neurol Neurosurg Psychiatry* **78**, 944-948, doi:10.1136/jnnp.2006.097154 (2007).

21 Jankovic, J. Parkinson's disease therapy: tailoring choices for early and late disease, young and old patients. *Clin Neuropharmacol* **23**, 252-261 (2000).

22 Brooks, D. J. Dopamine agonists: their role in the treatment of Parkinson's disease. *J Neurol Neurosurg Psychiatry* **68**, 685-689 (2000).

23 Pact, V. & Giduz, T. Mirtazapine treats resting tremor, essential tremor, and levodopa-induced dyskinesias. *Neurology* **53**, 1154 (1999).

24 Kordower, J. H. *et al.* Delivery of neurturin by AAV2 (CERE-120)-mediated gene transfer provides structural and functional neuroprotection and neurorestoration in MPTP-treated monkeys. *Ann Neurol* **60**, 706-715, doi:10.1002/ana.21032 (2006).

25 Gash, D. M., Zhang, Z. & Gerhardt, G. Neuroprotective and neurorestorative properties of GDNF. *Ann Neurol* **44**, S121-125 (1998).

26 Stover, N. P. *et al.* Intrastriatal implantation of human retinal pigment epithelial cells attached to microcarriers in advanced Parkinson disease. *Arch Neurol* **62**, 1833-1837, doi:10.1001/archneur.62.12.1833 (2005).

27 Recchia, A. *et al.* Alpha-synuclein and Parkinson's disease. *FASEB J* **18**, 617-626, doi:10.1096/fj.03-0338rev (2004).

28 Gomez-Tortosa, E. *et al.* Clinical and quantitative pathologic correlates of dementia with Lewy bodies. *Neurology* **53**, 1284-1291 (1999).

29 Volpicelli-Daley, L. A., Luk, K. C. & Lee, V. M. Addition of exogenous alpha-synuclein preformed fibrils to primary neuronal cultures to seed recruitment of endogenous alpha-synuclein to Lewy body and Lewy neurite-like aggregates. *Nat Protoc* **9**, 2135-2146, doi:10.1038/nprot.2014.143 (2014).

30 Kahle, P. J., Haass, C., Kretzschmar, H. A. & Neumann, M. Structure/function of alpha-synuclein in health and disease: rational development of animal models for Parkinson's and related diseases. *J Neurochem* **82**, 449-457 (2002).

31 Davidson, W. S., Jonas, A., Clayton, D. F. & George, J. M. Stabilization of alpha-synuclein secondary structure upon binding to synthetic membranes. *The Journal of biological chemistry* **273**, 9443-9449 (1998).

32 Clayton, D. F. & George, J. M. Synucleins in synaptic plasticity and neurodegenerative disorders. *J Neurosci Res* **58**, 120-129 (1999).

33 el-Agnaf, O. M. & Irvine, G. B. Aggregation and neurotoxicity of alpha-synuclein and related peptides. *Biochem Soc Trans* **30**, 559-565, doi:10.1042/ (2002).

34 George, J. M. The synucleins. *Genome Biol* **3**, REVIEWS3002 (2002).

35 Souza, J. M., Giasson, B. I., Chen, Q., Lee, V. M. & Ischiropoulos, H. Dityrosine cross-linking promotes formation of stable alpha -synuclein polymers. Implication of nitrative and oxidative stress in the pathogenesis of neurodegenerative synucleinopathies. *J Biol Chem* **275**, 18344-18349, doi:10.1074/jbc.M000206200 (2000).

36 Negro, A., Brunati, A. M., Donella-Deana, A., Massimino, M. L. & Pinna, L. A. Multiple phosphorylation of alpha-synuclein by protein tyrosine kinase Syk prevents eosin-induced aggregation. *FASEB J* **16**, 210-212, doi:10.1096/fj.01-0517fje (2002).

37 Crowther, R. A., Jakes, R., Spillantini, M. G. & Goedert, M. Synthetic filaments assembled from C-terminally truncated alpha-synuclein. *FEBS Lett* **436**, 309-312 (1998).

38 Chen, Y. G. *et al.* Phospholipase D stimulates release of nascent secretory vesicles from the trans-Golgi network. *J Cell Biol* **138**, 495-504 (1997).

39 Abeliovich, A. *et al.* Mice lacking alpha-synuclein display functional deficits in the nigrostriatal dopamine system. *Neuron* **25**, 239-252 (2000).

40 Ostrerova, N. *et al.* alpha-Synuclein shares physical and functional homology with 14-3-3 proteins. *J Neurosci* **19**, 5782-5791 (1999).

41 McNaught, K. S., Belizaire, R., Isacson, O., Jenner, P. & Olanow, C. W. Altered proteasomal function in sporadic Parkinson's disease. *Experimental neurology* **179**, 38-46 (2003).

42 Alberts, B. *Molecular biology of the cell*. 5th edn, (Garland Science, 2008).

43 Voges, D., Zwickl, P. & Baumeister, W. The 26S proteasome: a molecular machine designed for controlled proteolysis. *Annu Rev Biochem* **68**, 1015-1068, doi:10.1146/annurev.biochem.68.1.1015 (1999).

44 Hashimoto, M. *et al.* Oxidative stress induces amyloid-like aggregate formation of NACP/alpha-synuclein in vitro. *Neuroreport* **10**, 717-721 (1999).

45 Ostrerova-Golts, N. *et al.* The A53T alpha-synuclein mutation increases iron-dependent aggregation and toxicity. *J Neurosci* **20**, 6048-6054 (2000).

46 Jenner, P. & Olanow, C. W. Understanding cell death in Parkinson's disease. *Ann Neurol* **44**, S72-84 (1998).

47 Dawson, T., Mandir, A. & Lee, M. Animal models of PD: pieces of the same puzzle? *Neuron* **35**, 219-222 (2002).

48 White, R. R., Sullenger, B. A. & Rusconi, C. P. Developing aptamers into therapeutics. *J Clin Invest* **106**, 929-934, doi:10.1172/JCI11325 (2000).

49 Keefe, A. D., Pai, S. & Ellington, A. Aptamers as therapeutics. *Nature reviews. Drug discovery* **9**, 537-550, doi:10.1038/nrd3141 (2010).

50 Cheng, C., Chen, Y. H., Lennox, K. A., Behlke, M. A. & Davidson, B. L. In vivo SELEX for Identification of Brain-penetrating Aptamers. *Mol Ther Nucleic Acids* **2**, e67, doi:10.1038/mtna.2012.59 (2013).

51 Tuerk, C. & Gold, L. Systematic evolution of ligands by exponential enrichment: RNA ligands to bacteriophage T4 DNA polymerase. *Science* **249**, 505-510 (1990).

52 Tsukakoshi, K., Abe, K., Sode, K. & Ikebukuro, K. Selection of DNA aptamers that recognize alpha-synuclein oligomers using a competitive screening method. *Anal Chem* **84**, 5542-5547, doi:10.1021/ac300330g (2012).

53 Kolpashchikov, D. M. A binary deoxyribozyme for nucleic acid analysis. *Chembiochem : a European journal of chemical biology* **8**, 2039-2042, doi:10.1002/cbic.200700384 (2007).

54 Kolpashchikov, D. M. Binary probes for nucleic acid analysis. *Chemical reviews* **110**, 4709-4723, doi:10.1021/cr900323b (2010).

55 Cox, A. J., Bengtson, H. N., Rohde, K. H. & Kolpashchikov, D. M. DNA nanotechnology for nucleic acid analysis: multifunctional molecular DNA machine for RNA detection. *Chemical communications* **52**, 14318-14321, doi:10.1039/c6cc06889h (2016).

56 Ni, X., Castanares, M., Mukherjee, A. & Lupold, S. E. Nucleic acid aptamers: clinical applications and promising new horizons. *Current medicinal chemistry* **18**, 4206-4214 (2011).

57 Healy, J. M. *et al.* Pharmacokinetics and biodistribution of novel aptamer compositions. *Pharmaceutical research* **21**, 2234-2246 (2004).

58 Ruckman, J. *et al.* 2'-Fluoropyrimidine RNA-based aptamers to the 165-amino acid form of vascular endothelial growth factor (VEGF165). Inhibition of receptor binding and VEGF-induced vascular permeability through interactions requiring the exon 7-encoded domain. *The Journal of biological chemistry* **273**, 20556-20567 (1998).

59 Biesecker, G., Dihel, L., Enney, K. & Bendele, R. A. Derivation of RNA aptamer inhibitors of human complement C5. *Immunopharmacology* **42**, 219-230 (1999).

60 Meng, L. *et al.* Targeted delivery of chemotherapy agents using a liver cancer-specific aptamer. *PloS one* **7**, e33434, doi:10.1371/journal.pone.0033434 (2012).

61 Shi, H. *et al.* Au@Ag/Au nanoparticles assembled with activatable aptamer probes as smart "nano-doctors" for image-guided cancer thermotherapy. *Nanoscale* **6**, 8754-8761, doi:10.1039/c4nr01927j (2014).

62 Poduslo, J. F., Curran, G. L. & Berg, C. T. Macromolecular permeability across the blood-nerve and blood-brain barriers. *Proceedings of the National Academy of Sciences of the United States of America* **91**, 5705-5709 (1994).

63 Niewoehner, J. *et al.* Increased brain penetration and potency of a therapeutic antibody using a monovalent molecular shuttle. *Neuron* **81**, 49-60, doi:10.1016/j.neuron.2013.10.061 (2014).

64 Porciani, D. *et al.* Two interconvertible folds modulate the activity of a DNA aptamer against transferrin receptor. *Mol Ther Nucleic Acids* **3**, e144, doi:10.1038/mtna.2013.71 (2014).

65 Tian, X. *et al.* LRP-1-mediated intracellular antibody delivery to the Central Nervous System. *Sci Rep* **5**, 11990, doi:10.1038/srep11990 (2015).

66 Ellgaard, L. & Ruddock, L. W. The human protein disulphide isomerase family: substrate interactions and functional properties. *EMBO reports* **6**, 28-32, doi:10.1038/sj.embor.7400311 (2005).

67 Hatahet, F. & Ruddock, L. W. Substrate recognition by the protein disulfide isomerases. *The FEBS journal* **274**, 5223-5234, doi:10.1111/j.1742-4658.2007.06058.x (2007).

68 Turano, C., Coppari, S., Altieri, F. & Ferraro, A. Proteins of the PDI family: unpredicted non-ER locations and functions. *Journal of cellular physiology* **193**, 154-163, doi:10.1002/jcp.10172 (2002).

69 Fu, X. M. & Zhu, B. T. Human pancreas-specific protein disulfide-isomerase (PDIp) can function as a chaperone independently of its enzymatic activity by forming stable complexes with denatured substrate proteins. *The Biochemical journal* **429**, 157-169, doi:10.1042/BJ20091954 (2010).

70 Grek, C. & Townsend, D. M. Protein Disulfide Isomerase Superfamily in Disease and the Regulation of Apoptosis. *Endoplasmic reticulum stress in diseases* **1**, 4-17, doi:10.2478/ersc-2013-0001 (2014).

71 Wang, L., Wang, X. & Wang, C. C. Protein disulfide-isomerase, a folding catalyst and a redox-regulated chaperone. *Free Radic Biol Med* **83**, 305-313, doi:10.1016/j.freeradbiomed.2015.02.007 (2015).

72 Jessop, C. E., Watkins, R. H., Simmons, J. J., Tasab, M. & Bulleid, N. J. Protein disulphide isomerase family members show distinct substrate specificity: P5 is targeted to BiP client proteins. *J Cell Sci* **122**, 4287-4295, doi:10.1242/jcs.059154 (2009).

73 Xu, S., Sankar, S. & Neamati, N. Protein disulfide isomerase: a promising target for cancer therapy. *Drug Discov Today* **19**, 222-240, doi:10.1016/j.drudis.2013.10.017 (2014).

74 Perri, E. R., Thomas, C. J., Parakh, S., Spencer, D. M. & Atkin, J. D. The Unfolded Protein Response and the Role of Protein Disulfide Isomerase in Neurodegeneration. *Front Cell Dev Biol* **3**, 80, doi:10.3389/fcell.2015.00080 (2015).

75 Walker, A. K. Protein disulfide isomerase and the endoplasmic reticulum in amyotrophic lateral sclerosis. *J Neurosci* **30**, 3865-3867, doi:10.1523/JNEUROSCI.0408-10.2010 (2010).

76 Hetz, C. The unfolded protein response: controlling cell fate decisions under ER stress and beyond. *Nat Rev Mol Cell Biol* **13**, 89-102, doi:10.1038/nrm3270 (2012).

77 Rutkowski, D. T. *et al.* Adaptation to ER stress is mediated by differential stabilities of pro-survival and pro-apoptotic mRNAs and proteins. *PLoS Biol* **4**, e374, doi:10.1371/journal.pbio.0040374 (2006).

78 Halperin, L., Jung, J. & Michalak, M. The many functions of the endoplasmic reticulum chaperones and folding enzymes. *IUBMB Life* **66**, 318-326, doi:10.1002/iub.1272 (2014).

79 Schroder, M. & Kaufman, R. J. ER stress and the unfolded protein response. *Mutat Res* **569**, 29-63, doi:10.1016/j.mrfmmm.2004.06.056 (2005).

80 Cao, S. S. & Kaufman, R. J. Unfolded protein response. *Curr Biol* **22**, R622-626, doi:10.1016/j.cub.2012.07.004 (2012).

81 Lee, A. H., Iwakoshi, N. N. & Glimcher, L. H. XBP-1 regulates a subset of endoplasmic reticulum resident chaperone genes in the unfolded protein response. *Mol Cell Biol* **23**, 7448-7459 (2003).

82 Ma, Y. & Hendershot, L. M. ER chaperone functions during normal and stress conditions. *J Chem Neuroanat* **28**, 51-65, doi:10.1016/j.jchemneu.2003.08.007 (2004).

83 Soo, K. Y., Atkin, J. D., Horne, M. K. & Nagley, P. Recruitment of mitochondria into apoptotic signaling correlates with the presence of inclusions formed by amyotrophic lateral sclerosis-associated SOD1 mutations. *J Neurochem* **108**, 578-590, doi:10.1111/j.1471-4159.2008.05799.x (2009).

84 Benhar, M., Forrester, M. T. & Stamler, J. S. Nitrosative stress in the ER: a new role for S-nitrosylation in neurodegenerative diseases. *ACS Chem Biol* **1**, 355-358, doi:10.1021/cb600244c (2006).

85 Outeiro, T. F. *et al.* Formation of toxic oligomeric alpha-synuclein species in living cells. *PloS one* **3**, e1867, doi:10.1371/journal.pone.0001867 (2008).